UNIVERSITY OF CALIFORNIA, SAN DIEGO

Design and Synthesis of Ligands Targeting the Hepatitis C Virus Internal Ribosome Entry Site

A Thesis submitted in partial satisfaction of the requirements for the degree

Master of Science

in

Chemistry

by

Brian P. Charrette

Committee in charge:

Professor Thomas Hermann, Chair
Professor Emmanuel Theodorakis
Professor Navtej Toor

2016

The Thesis of Brian P. Charrette is approved, and it is acceptable in quality and form for publication on microfilm and electronically:

_____

_____

_____

Chair

University of California, San Diego

2016

DEDICATION

I would like to dedicate my thesis to my amazing partner Kaleen, whose constant love and support is the reason this thesis was completed and I owe her so much. The sacrifices she made for my success during the good and bad cannot be expressed enough and she has always had my back. I am so grateful to have you in my life every day.

I would like to dedicate this thesis to my family. My mom and dad always encouraged me to strive to be better and never give up even in hard times. My brothers Aaron, James, and Jared have been there to support me since day one.

I would also like to thank my advisor, Prof. Thomas Hermann, who has been an incredible mentor for me. His genuine interest to develop me into a better scientist and person is humbling and I could not have done this without his help.

I want to thank my coworkers in the Hermann Lab over the years, Kevin Rynearson and Erik Romero were instrumental in helping my synthesis, and Mark Boerneke helped me with the biochemistry assays. Sergey Dibrov, Gloria Torres, Keija Ding, Quint Frauman, Leena Oubeid, Shi Chen, Zihao Wang, and Eileen Tran thank you all for your help.

TABLE OF CONTENTS

LIST OF FIGURES

LIST OF TABLES

LIST OF SCHEMES

LIST OF SPECTRA

ACKNOWLEDGEMENTS

I would like to thank Professor Thomas Hermann for his immeasurable guidance throughout my time here at UCSD. Always willing to listen, he has taught me to think critically to solve problems and never give up. I am honored and extremely grateful to have worked in his lab.

I am very grateful of Dr. Yongxuan Su (UCSD MS Facility) for his assistance with all of the mass spectrometry measurements. I also want to thank Dr. Anthony Mrse for his help and training using the NMR instruments (UCSD NMR Facility). Thanks to Dr. Kevin Rynearson for all of the help when I first came to Hermann's Lab and continued until I finished my M.S.

The material in the Introduction, in part, have been published in Bioorganic & Medicinal Chemistry Letters (**2014**, 24, 3521-3525) titled *2-Aminobenzoxazole ligands of the hepatitis C virus internal ribosome entry site* with Kevin Rynearson, Christopher Gabriel, Jesus Moreno, Mark Boerneke, Sergey Dibrov, and Thomas Hermann as co-authors. The thesis author is the second author on this paper.

ABSTRACT OF THE THESIS

Design and Synthesis of Ligands Targeting the Hepatitis C Virus Internal Ribosome Entry Site

by

Brian P. Charrette

Master of Science in Chemistry

University of California, San Diego, 2016

Professor Thomas Hermann, Chair

Benzodiazepinones and cyclopropylquinazolinamines were designed and synthesized with the goal of creating ligands for the subdomain IIa of the hepatitis C virus (HCV) internal ribosome entry site (IRES) RNA and thereby

inhibiting viral translation. The heterocyclic scaffolds were designed using insight into molecular recognition of the RNA target by previously discovered synthetic and natural ligands. The novel benzodiazepinones and cyclopropylquinazolinamines were evaluated for RNA target binding by a previously developed FRET assay.

Design and Synthesis of Ligands Targeting the Hepatitis C Virus Internal Ribosome Entry Site

Introduction

1.1 RNA as a drug target

RNA's role in biology has been thoroughly studied over the last few decades for the many key processes that it participates in throughout all living organisms. Although RNA was traditionally known for its main role of transferring genetic information as messenger RNA (mRNA) from DNA during translation to proteins, mRNA accounts only for a small fraction of the roles RNA plays. A large portion of RNA is non-coding (ncRNA)[1] which may form complex three-dimensional structures, undergoing specific and unique conformational changes, interacting with proteins, other nucleic acids and metabolites. The wide range of ncRNA biological functions has inspired research on small molecules as modulators of ncRNA which offer a diverse structural scaffold for interactions including hydrogen bonding and pi stacking. Unlike proteins which may carry both positive and negative charged amino acid residues, RNA surfaces are limited to regions of negative charge due to the acidic character of the nucleotide building blocks. Small molecules tailored to accommodate these structural features of ncRNA can bind and thereby affect conformations and ultimately function of ncRNA. Despite the rich diversity of possible binding in folded RNA, such ncRNA targets are yet underexplored for small molecule inhibition. As an exception, many antibiotics target ribosomal RNA, including clinically important drugs such as oxazolidinones, macrolides, tetracyclins, and aminoglycosides.[2] Nevertheless, targeting ncRNA has proven difficult. Some previously studied RNA targets include the human immunodeficiency virus

(HIV) trans-activation response (TAR) element, Rev-response element (RRE),[3] and the hepatitis C virus (HCV) internal ribosome entry site (IRES),[4] and several bacterial riboswitches.[5] One of the main challenges for developing ligands for an ncRNA arises from ligand specificity. While ncRNA elements in viral genomes are highly conserved and play essential roles in the viral infection cycle, similar RNAs are absent in human, and therefore development of selective viral inhibitors may be feasible. Targeting these non-coding viral RNA regions could lead to effective therapeutics that could have a high barrier to resistant mutant emergence.[4]

1.2 Hepatitis C Virus

HCV is a well-known viral pathogen that primarily targets the liver and is the leading cause for liver transplants worldwide.[6],[7] HCV infection leads to cirrhosis or hepatocellular carcinoma several years after the initial infection.[8] Infection with HCV is widespread, with of ~150 million people affected worldwide including 3-4 million patients in the USA, and causing ~300,000 deaths each year from HCV-induced liver disease.[9],[10] With 3-4 million new patient diagnoses every year, a higher mortality rate than HIV in the USA,[11] and no effective current vaccine, HCV infection represents an urgent medical need for the development of antiviral therapies. The virus is bloodborne, and infection is now most common through unsafe needle/injection drug use. In the last few years, several direct acting antivirals for HCV have been introduced into the

clinic which achieve viral cure rates of greater than 90%.[12] Several antivirals were approved in which inhibit viral protease, RNA polymerase, or the nonstructural protein NS5A replication complex.[13],[14] The standard treatment before this recent therapies for HCV was repeated injection with polyethylene glycol-conjugated (“pegylated”) interferons in combination with the small molecule drug ribavirin, which often resulted in serious side effects, poor patient compliance and limited efficacy.[15],[16] Since HCV clinical isolates show genetic variants, HCV quasispecies, and preexisting drug resistant mutations, it is challenging to develop a universal cure and additional agents are often required to treat the virus infection through combination therapy.[17],[7] As a result, our lab is interested in discovering inhibitors of viral ncRNA for the development of novel treatments that target the virus in a unique way and which could be used to target all viral genotypes.

1.3 IRES RNA target in Hepatitis C

The HCV virus belongs to the *Hepacivirus* genus and *Flaviviridae* family of viruses and contains a single-stranded, positive-sense RNA genome.[18] It consists of 9379 nucleobases, flanked by two untranslated regions (5’- and 3’-UTR) which are critical to viral translation and replication (**Figure 1.3.1**).[19],[20]

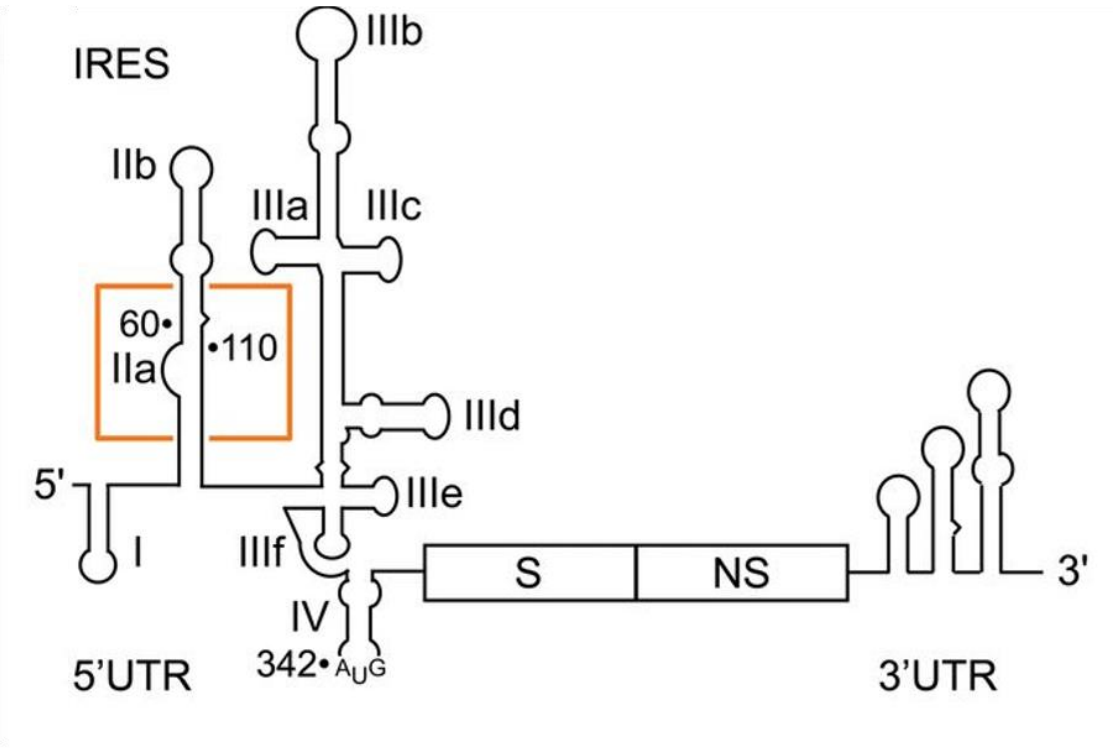

Figure 1.3.1: The Hepatitis C virus (HCV) genome. The highly conserved and complex internal ribosome entry site (IRES) is in the 5' untranslated region (UTR). The open reading frame (ORF) encodes 3 structural and 7 nonstructural proteins. The AUG start codon resides in the IRES domain IV hairpin which unwinds during translation initiation. The genome also contains a structured 3' UTR. The region in the gold box is the subdomain IIa. Figure modified from ref[1], 2015, Macmillan Publishers Limited.

The viral genome is used directly as the messenger RNA (mRNA) coding for viral proteins and serving as a template for replication. Between the untranslated regions is the open reading frame which encodes 3 structural and 7 nonstructural viral proteins. The IRES in particular has been found nearly fully conserved in HCV clinical isolates and is required for the translation of viral proteins. Cryo-Electron microscopy studies of the HCV IRES in complex with

ribosome have revealed the IRES structure bound to the 40S ribosomal subunit (**Figure 1.3.2**).[21]

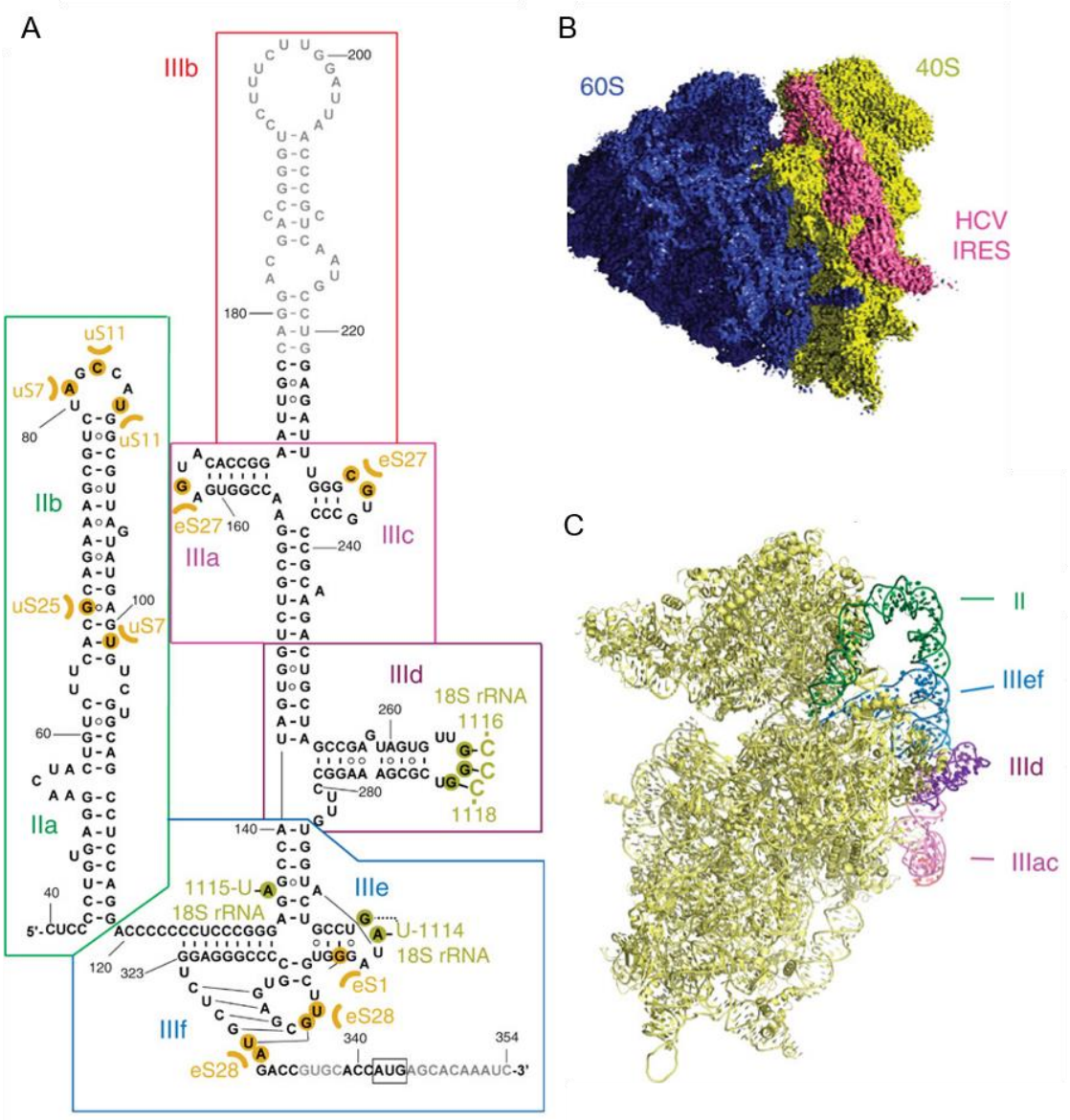

Figure 1.3.2: Cryo-EM results of HCV IRES and human ribosome. A) secondary structure of the HCV IRES. The domains are indicated by color and roman numerals. Canonical base pairs are connected via lines, where non-standard base pairs are shown with circles between them. Interactions with the ribosomal proteins are in orange, and interactions with the 18S rRNA are in dark yellow. The bases in grey were not used to construct the actual structure for the Cryo-EM study, and the start codon is boxed in black. B) EM density of 80S-HCV IRES complex, note the IRES does not contact the 60S ribosome subunit. 40S ribosomal subunit is in yellow, 60S in blue, and HCV IRES in pink. C) Side view of the structure of the HCV IRES bound to the human 40S. Figure modified from ref[1], 2015, Macmillan Publishers Limited.

The IRES domain II, which is comprised of sub-domains IIa and IIb, has been shown to be integral in binding the viral IRES to the 40S ribosomal subunit for translation of the viral RNA to occur.[22],[23],[24],[25] Deletion of domain II, or IIa and IIb individually prevents the IRES from initiating translation while binding to the 40S subunit is still possible.[26] More specifically, the bent fold of subdomain IIa is critical to the placement of the domain IIb hairpin during translational initiation (**Figure 1.3.3**).[26] Due to its importance in translation and near full conservation across clinical isolates, the subdomain IIa has been proposed as a target for the discovery of new antiviral drugs.

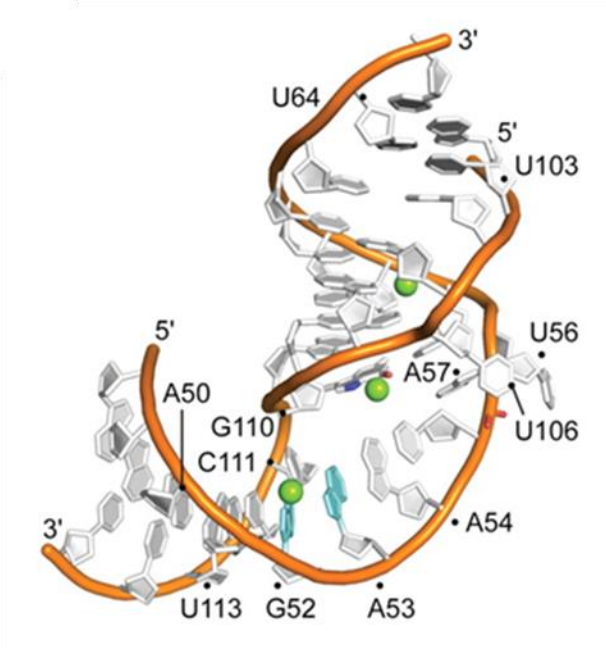

Figure 1.3.3: Crystal structure of the subdomain IIa of the HCV IRES. Backbone in orange, green spheres are Mg^{2+} ions. The nearly 90° turn in 3D structure is key to placing the subdomain IIb hairpin in the correct position to recruit the 40S ribosome and initiate translation. Image was prepared from PDB coordinate file 2NOK.

The IRES RNA in the HCV genome initiates translation of viral proteins in a cap-independent process by hijacking host cell ribosomes and eliminating the need for most host initiation factors (**Figure 1.3.4**).

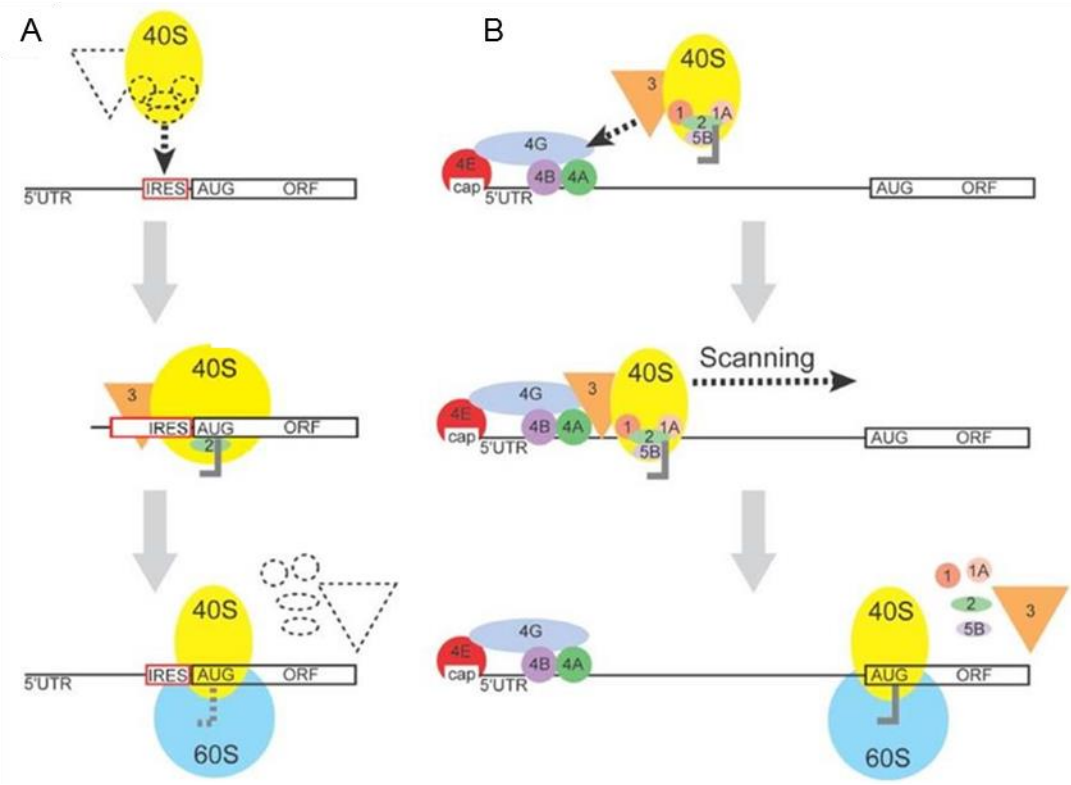

Figure 1.3.4: Mechanisms for eukaryotic translation initiation. A) IRES mediated translation initiation, which does not require a cap structure (cap), involves direct binding of the 40S ribosomal subunit, requires no 40S scanning, or many of the initiation factors (shown in dotted shaped outlines) required for eukaryotic translation initiation. B) Cap-dependent eukaryotic translation mechanism, requiring a cap structure, several initiation factors (colored shapes 4A, 4B, 4E, 4G, 1, 1A, 2, 3, and 5B) and 40S ribosomal scanning to the start codon for translation initiation. Figure modified from ref[27], 2012, John Wiley & Sons Ltd.

Due to the key role the HCV IRES plays in viral translation, inhibition of the IRES RNA presents an attractive target for antiviral drug therapy.

Previously discovered compounds such as **1** and **2** (**Figure 1.3.5**) have been shown to inhibit translation of HCV by binding to the HCV IRES subdomain IIa.[7]

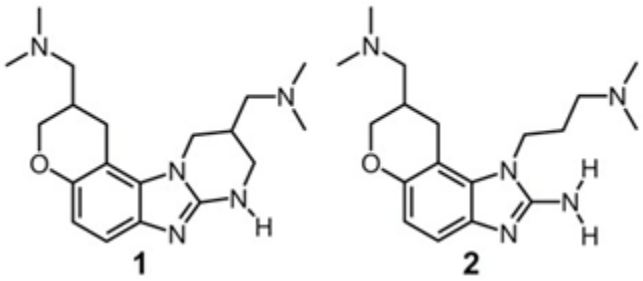

Figure 1.3.5: The highly substituted benzimidazole inhibitors **1** and **2**. Originally synthesized by Ionis Pharmaceuticals.[7],[28]

Compounds of the benzimidazole series which had initially been synthesized at Ionis Pharmaceuticals, form key hydrogen bonds to G110 and C58 bases, as seen in the co-crystal structure of compound **2** bound to the HCV IRES (**Figure 1.3.6**). Loss of the ability to hydrogen bond to these base pairs, as in derivatives having a carbonyl or methyl group (**Figure 1.3.7**), results in complete loss of binding affinity of the compound to the IRES RNA target.

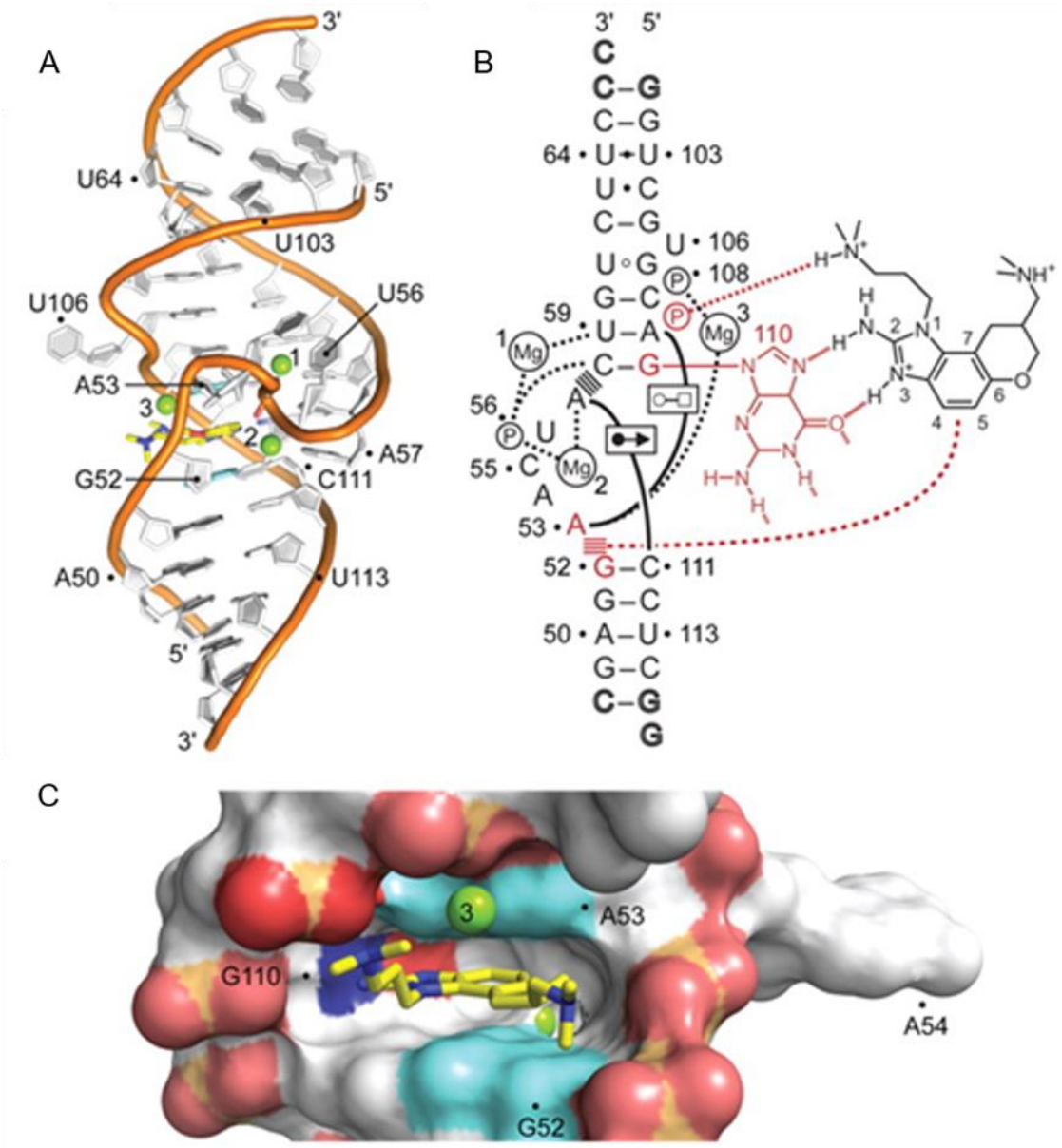

Figure 1.3.6: Crystal structure of subdomain IIa with bound benzimidazole inhibitor **2**. A) Co-crystal structure of domain IIa and inhibitor **2** as it captures the IRES in an elongated form, inhibiting viral translation. Inhibitor **2** is shown in yellow. B) Overview of the specific interactions in the binding pocket with compound **2**. Hydrogen bonds are shown as dashed lines, and the formation of non-Watson-Crick base pairs are indicated with lines and symbols according to ref #. Residue interactions between **2** and base pairs are indicated in red. Stacked lines (≡) represent stacking of bases and intercalation of the ligand. C) Surface representation model, to highlight the deep binding pocket. Figure modified from ref[7], 2012, PNAS Ltd.

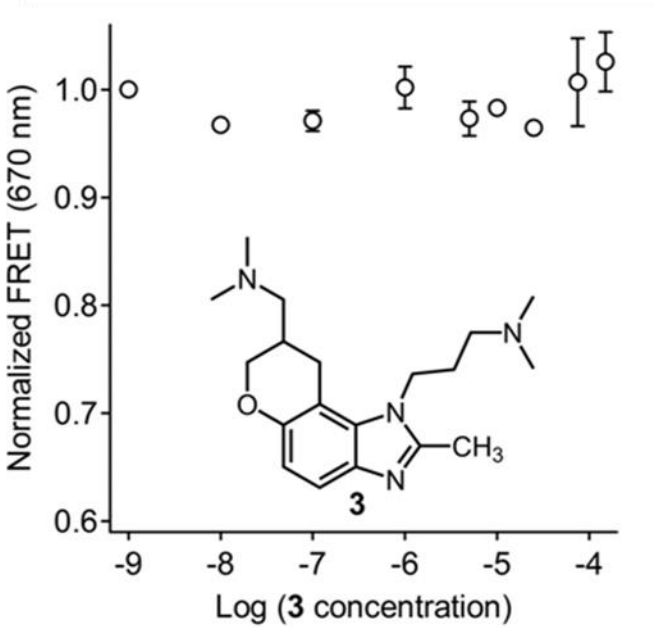

Figure 1.3.7: FRET assay of compound **3**. Normalized FRET readings at 670 nm plotted against the Log of the concentration of **3**, at increasing concentrations of **3** in triplicate. Error bars represent ± 1 standard deviation (SD) calculated from the three independent titrations. Figure modified from ref[7], 2012, PNAS Ltd.

1.4 FRET binding assay for HCV IRES

Due to the important role that domain II plays in viral translation, compounds that bind to this region and disturb the native RNA folding could lead to HCV inhibitor drugs. To test compounds for binding at the subdomain IIa RNA target, a Förster Resonance Energy Transfer (FRET) Assay was designed. Guided by the crystal structure of the subdomain IIa, a pair of cyanine dyes was attached at the 5'-termini (Cy3 and Cy5) of the RNA target (**Figure 1.4.1A**). The RNA construct design placed the FRET dyes in a distance close to the Förster radius and allowed sensitive monitoring of conformational changes in the RNA.[29],[30]

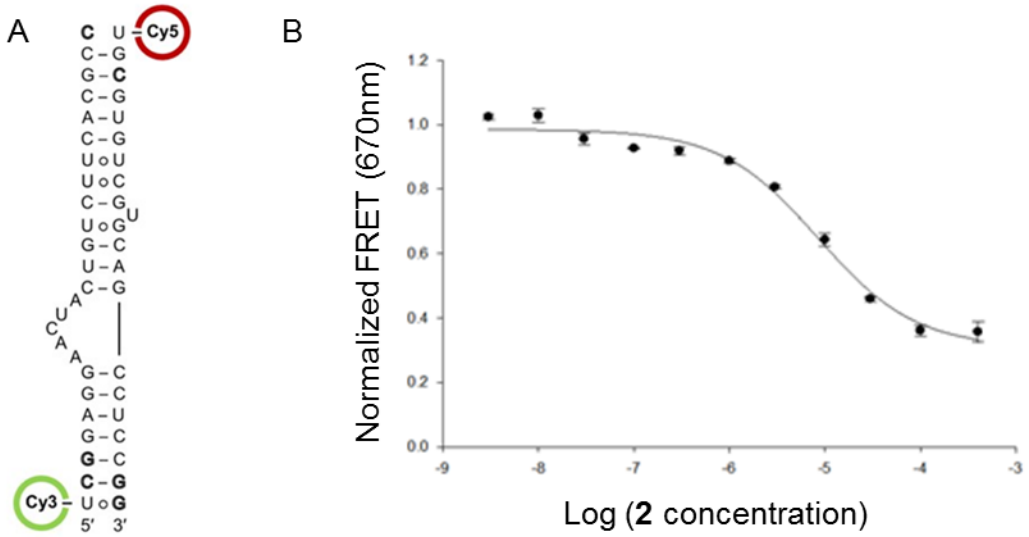

Figure 1.4.1: The RNA FRET assay. A) Structure and sequence of dye-labeled HCV IRES subdomain IIa construct for the FRET assay.[29][31] B) Observed normalized FRET signal with increasing concentration of benzimidazole inhibitor **2** in the presence of 2mM Mg^{2+} ions.[29]

The FRET effect (**Figure 1.4.2**) is proportional to the inverse 6th power of the distance between the two chromophores, which leads to small changes to the dye distance giving rise to large FRET signal changes.

$$E = \frac{1}{1 + \left(\frac{r}{R_o}\right)^6}$$

Figure 1.4.2: The Förster Resonance Energy Transfer equation. E is the FRET efficiency, or the fraction of energy transfer per donor excitement. r is the actual distance the two chromophores are from each other at any given time in, and R_o is the Förster distance of the particular pair of chromophores, Cy3 and Cy5 in our case, where R_o is 56 Å.

A FRET signal is not observed in the absence of divalent metal ions, such as Mg2+, as the internal loop of subdomain IIa requires metal ions for stable

folding. In the unfolded state of the RNA, the cyanine dyes are placed outside of the Förster radius, giving no FRET. However, the addition of Mg2+ ions yields a dose-dependent increase of the FRET signal due to the stable folding of the subdomain IIa which brings the cyanine dyes in optimal FRET distance. Compounds that can distort proper folding or change the native conformation of subdomain IIa should result in a changed FRET signal compared to the native fold of subdomain IIa. Addition of the known translational inhibitor 2 in the presence of 2mM Mg2+ ions resulted in dose-dependent quenching of the FRET signal, which suggests that the ligand 2 captures the subdomain IIa in a form that is elongated or distorted and thereby places the cyanine dyes outside of the Förster radius (**Figure 1.4.1A**). Since the FRET signal change is dose-dependent, and different ligands have distinct affinity in binding to the RNA, the FRET assay allows an efficient way to compare binding of various small molecule ligands. A measure for ligand binding affinity determined by this FRET assay is the EC_{50} value, which is derived from the ligand concentration at which the compound causes 50% inhibition or binding to the target (subdomain IIa RNA).

1.5 Previous targets to HCV IRES

The benzimidazoles found to bind to the HCV IRES were initially discovered by Ionis Pharmaceuticals by means of a mass spectrometry-based high throughput screen against the IRES RNA. The screen identified the

aminobenzimidazole 4 as a hit with a binding affinity of around 100 µM (**Figure 1.5.1**).[28]

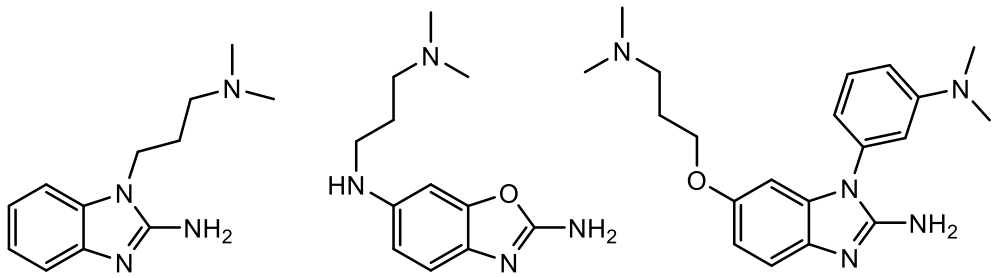

4 **5** **6**

Figure 1.5.1: 1-(3-(dimethylamino)propyl)-1H-benzo[d]imidazol-2-amine **4** shown to be one of the best hits on the high throughput screening of compounds done by Ionis Pharmaceuticals.[28] Benzoxazole N6-(3-(dimethylamino)propyl)benzo[d]oxazole-2,6-diamine **5**, which has an EC_{50} of 25 µM and 1-(3-(dimethylamino)phenyl)-6-(3-(dimethylamino)propoxy)-1H-benzo[d]imidazol-2-amine **6**, which has an EC_{50} of 103 µM.

Using the FRET IRES construct as a guide to compare relative EC_{50} values, compounds were designed to optimize the interaction of benzimidazole derivatives with the IRES. The best two compounds being 1 and 2, as described before, which showed binding at the IRES with EC_{50} values of 0.72 µM and 0.86µM respectively.[28] The main difference between the compounds is the side chain flexibility; the more rigid compound showed better binding. The compound **1** has a better EC_{50}, since its second side chain is less free to rotate and move around in solution. The main shortcoming of these compounds is the difficulty of their synthesis. For compound **2**, the synthesis had overall 13 steps and 4.9% overall yield; compound **1** had a 12 step 0.4% overall yield.[28] An effort to increase yields and reduce synthetic steps was attempted in our lab in

2011 to determine if access to this highly active compound could be improved. Although this work led to a shorter synthesis of **2**, with eight steps and a 10.7% overall yield,[32] this still was not efficient enough for larger scale synthesis of derivatives. A previous PhD student in our lab, Keija Ding, attempted to make several benzimidazole derivatives that used N1-coupled aryl substituents to achieve similar 'locking' of the side chain conformation and increase activity. Although the synthetic routes were more concise with higher yields, the binding activity was diminished.

With the benzimidazole inhibitors being nearly fully optimized, suffering from poor yield and long synthetic routes, and being fairly basic compounds with a pK_a around 7.5[33],[34] for the imidazole scaffold, our lab went on to design new compounds with more drug-like properties and straightforward synthetic routes. Kevin Rynearson, a previous PhD student in the lab, synthesized substituted benzoxazoles such as **5** (**Figure 1.5.1**)(**Table 1.5.1**) in whose synthesis I was involved with while being an undergraduate student researcher in the lab.[34]

Although these compounds were easier to synthesize with better yields and less steps, and the basicity of the compounds was less than that of the benzimidazoles, with a pK_a of the benzoxazoles being around 4.5,[33],[34] the binding activity was lower than that of the previously described benzimidazole inhibitors.

Table 1.5.1: Novel benzoxazoles synthesized in our group with binding affinity measured by the FRET assay. EC_{50} values are calculated from ligand binding curves of triplicate experiments (± 1 SD). EC_{50} is the concentration required for a fifty percent reduction in the observed FRET signal.

Structure	FRET
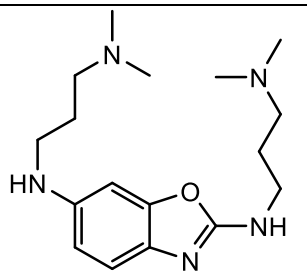	63 µM
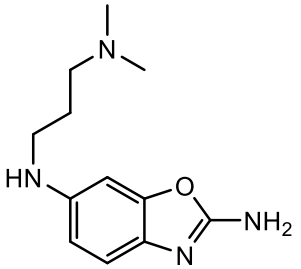	25 µM
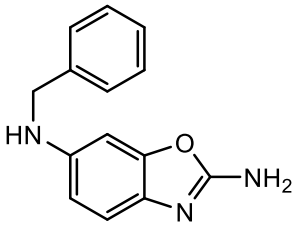	27 µM
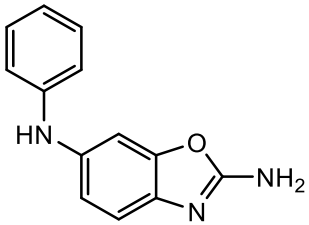	90 µM

The lower binding affinity was likely due to the lower basicity of the oxazoles which affected hydrogen bonding to the RNA target. The challenge achieving lower basicity in a drug-like compound combined with high affinity binding to the IRES may be difficult to achieve, as illustrated by scaffolds discussed above.

1.6 Guanine is a natural cognate ligand for the IRES subdomain IIa

Based on the crystal structure of benzimidazole inhibitor bound to the subdomain IIa RNA, and inspired by Yarus's classic study of arginine and guanine binding to self-splicing group I introns,[35] our lab proposed that the IRES subdomain IIa may be the target of a cognate biological ligand whose role may be that of facilitating release of the IRES from the ribosome. FRET testing was done on several derivatives of arginine and guanine (**Figure 1.6.1**), under the assumption that these molecules would engage in hydrogen bonding comparable to compounds such as **2** to the subdomain IIa region which involve two hydrogen bonds to the Hoogsteen edge of the G110-C58 base pair.

Figure 1.6.1: SAR study of guanine and structurally related compounds used for subdomain IIa binding testing in the FRET assay. Compounds include purines A1-A6, 2-amino-quinazoline derivatives B1-B9, pteridine derivatives C1-C5, tetrahydropteridine derivatives D1-D2, and dihydropteridine derivatives E1-E2. EC_{50} values are calculated using FRET dose response or Cy3 fluorescence response as indicated in parenthesis (FRET, Cy3) and are listed with ± 1 standard deviation calculated from triplicate experiments. No activity (n.a.) is listed for compounds which had no effect in the FRET assay. Compounds which precipitated RNA at concentrations used in the experiments are labelled as “precipitation.”

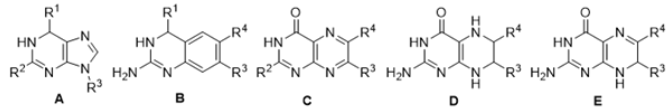

Compound	R^1	R^2	R^3	R^4	EC_{50}
A-1	=O	NH_2	H		1100 ± 100 (Cy3)
A-2	NH_2	NH_2	H		> 2000 (FRET)
A-3	$N(CH_3)_2$	NH_2	H		> 2000 (FRET)
A-4	=O	=O	H		n.a.
A-5	=O	NH_2			430 ± 340 (FRET)
A-6	=O	NH_2			1600 ± 4100 (FRET)
B-1	=O		H	H	480 ± 120 (Cy3)
B-2	NH_2		H	H	810 ± 2000 (Cy3)
B-3	H		H	H	precip.
B-4	NH_2		H	NH_2	precip.
B-5	=O		Cl	H	> 2000 (FRET)
B-6	=O			H	precip.
B-7	=O		C_6H_5	H	precip.
B-8	=O			H	precip.
B-9	=O			H	precip.
C-1		NH_2	H	H	> 2000 (Cy3)
C-2		NH_2	H		n.a.
C-3		NH_2	H		> 2000 (FRET)
C-4		OH	H	H	n.a.
C-5		OH		see R^3	precip.
C-6	NH_2	NH_2	H	CH_2OH	precip.
D-1			H		640 ± 50 (FRET)
D-2			CH_3	CH_3	1800 ± 2000 (FRET)
E-1			H		> 2000 (FRET)
E-2			=O	H	n.a.

Of the four natural nucelobases, only guanine showed activity, with an EC_{50} of about 1mM causing decrease of the FRET signal with increasing guanine concentration (**Figure 1.6.2**).

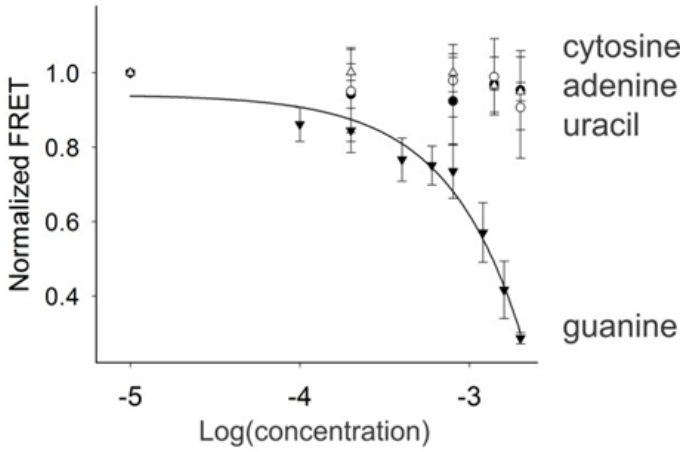

Figure 1.6.2: FRET dose response titration curve for all four natural nucleobases. Only guanine (▼) showed the dose-dependent drop in FRET signal with increasing concentration. Cytosine (●), adenine (○) and uracil (∆) showed no FRET change. Figure modified from ref[26], 2014, PNAS Ltd.

We hypothesized that the ribosome is initially recruited by the viral HCV IRES, followed by translation initiation that involves a G-residue that is liberated from a G-C pair during translation, which could bind to the subdomain IIa, trapping it in the elongated conformation, and detaching it from the ribosome in order to allow full translation and refolding of the IRES to complete the cycle (**Figure 1.6.3**).[26]

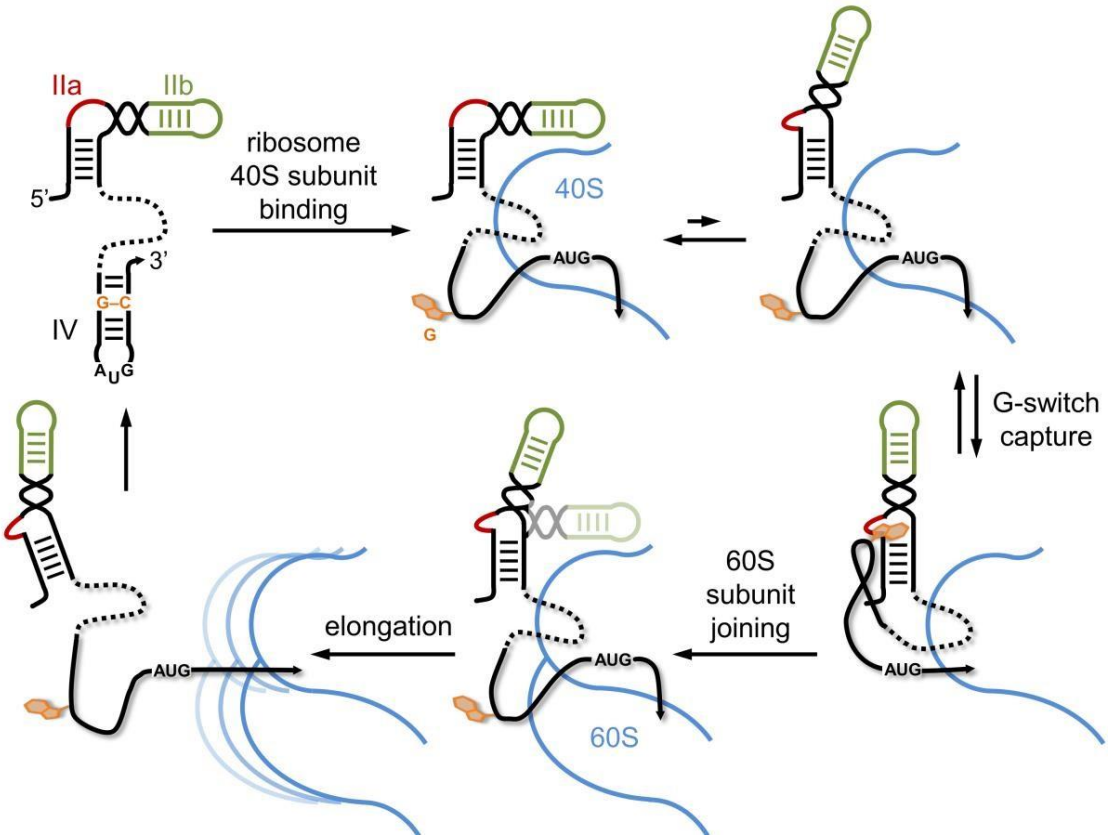

Figure 1.6.3: The proposed mechanism for the regulation of IRES activity by the subdomain IIa switch. through an interaction with a G residue from domain IV. Ribosome binding of the IRES entails melting of the domain IV hairpin to provide access of the viral start codon to the decoding site, which releases a G residue that facilitates functional IRES translation initiation by capture of the subdomain IIa extended conformation. This allows release of the IRES from the ribosome and refolding of the IRES to repeat the cycle anew. Figure modified from ref[26], 2014, PNAS Ltd.

The material in the Introduction, in part, have been published in Bioorganic & Medicinal Chemistry Letters (**2014**, 24, 3521-3525) titled *2-Aminobenzoxazole ligands of the hepatitis C virus internal ribosome entry site* with Kevin Rynearson, Christopher Gabriel, Jesus Moreno, Mark Boerneke,

Sergey Dibrov, and Thomas Hermann as co-authors. The thesis author is the second author on this paper.

Results and discussion

2.1 Design and Synthesis of other heterocycles targeting the HCV IRES subdomain IIa

The 2-aminoquinazolinone **7** had close to double the binding affinity compared to the natural guanine ligand, with an EC_{50} of 480 ± 120 µM, likely due to the benzene allowing favorable pi-stacking interactions and filling more space in the binding pocket than the guanine imidazole ring. The guanine and 2-aminoquinazolinone show similarities to the benzimidazole inhibitors (**Figure 2.1.1**) but have the advantage of being less basic.

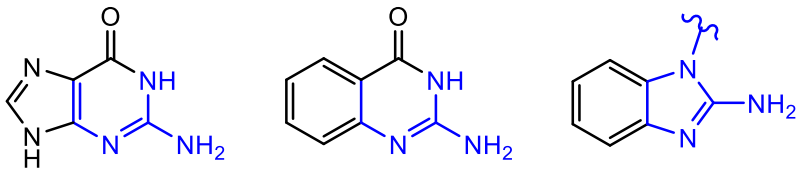

7 **4**

Figure 2.1.1: Guanine, 2-aminoquinazolinone **7**, and the benzimidazole **4**. Highlighted in blue is the shared scaffold to the core of benzimidazole **4**.

Based on the binding testing of the several guanine-like compounds with simple and complex substituents we decided to synthesize a guanine-like compound with the previously proven ligand side chain of N^1,N^1-dimethylpropyl-diamine found in compounds like **2** and test if FRET results would justify further optimization and exploration of the quinazolinone scaffold.

The synthesis of compounds **8** and **9** were previously performed by Ph.D. student Keija Ding and me (**Figure 2.1.2**).

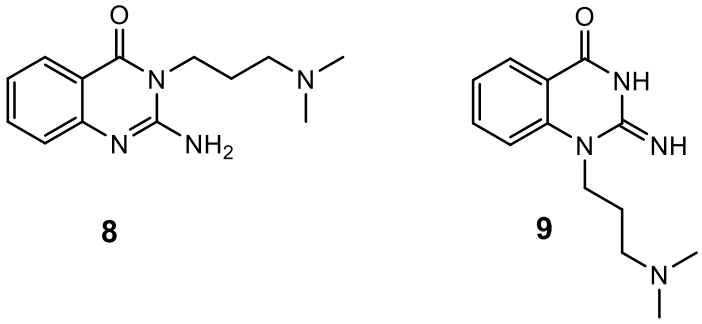

8 **9**

Figure 2.1.2: Previously synthesized compounds 2-amino-3-(3-(dimethylamino)propyl)quinazolin-4(3H)-one **8** and 1-(3-(dimethylamino)propyl)-2-imino-2,3-dihydroquinazolin-4(1H)-one **9**.

Compound **8** was previously synthesized using the N^1,N^1-dimethylpropyl-diamine and undergoing nucleophilic substitution to 2-nitrobenzoyl chloride. The nitro group was reduced with activated Palladium on carbon (Pd/C) and hydrogen gas to afford 2-amino-N-(3-(dimethylamino)propyl)benzamide. This was cyclized to **8** via nucleophilic substitution to cyanogen bromide, then intramolecular nucleophilic addition to close the ring when refluxed in acetonitrile giving compound **8** in 35% overall yield. Compound **9** proved much more difficult to synthesize as the starting material methyl 2-aminobenzoate proved to be a weak nucleophile and did not readily undergo nucleophilic substitution reactions with commercially available compounds like 3-chloro-N,N-dimethylpropan-1-amine. However, under Palladium (Pd/C) catalyzed Buchwald-Hartwig amination conditions with the aniline or nitro group, alkyl-nitrile, and hydrogen gas, the substitution was afforded at 56% yield (**Scheme 2.1.1**).[36]

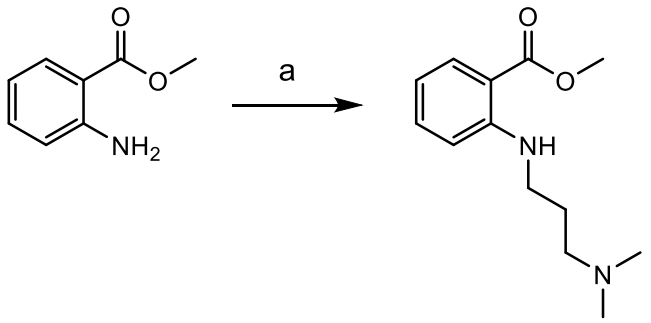

Scheme 2.1.1: synthesis of methyl 2-((3-(dimethylamino)propyl)amino) benzoate.

Reagents and conditions: Pd/C, H_2, 3-(dimethylamino)propanenitrile, MeOH, R.T., 24hr, 56%.[36]

Finally, cyclizing this with compound **10**, achieved via the addition of hydrochloric acid (HCl) to cyanamide, gave the final product **9** with 40% yield (**Scheme 2.1.2**).

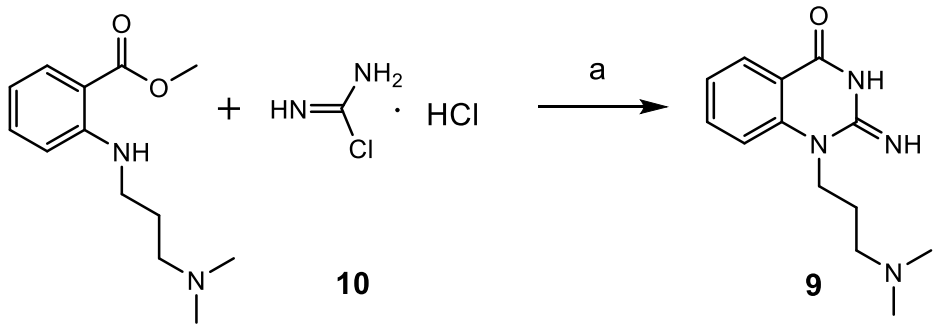

Scheme 2.1.2: Synthesis of quinazolinone **9**.

Reagents and conditions: Dimethylsulfone, 160 °C, 2hr, 40%.

At the same time, a previous postdoc in our lab, Dr. Gloria Torres, synthesized an interesting quinazolinone analog in which the carbonyl group was replaced with an SO_2 group instead, to determine if this larger and non-planar group would be accommodated by the HCV IRES target. These

compounds **11** and **12** as well as **8** and **9** were tested in FRET assay (**Table 2.1.1**).

Table 2.1.1: Compounds **8**, **9**, **11**, and **12** tested in the HCV IRES FRET assay. EC_{50} is the concentration required for a fifty percent reduction in the observed FRET signal. The term "n.a." means the EC_{50} couldn't be calculated as the signals were not fully saturated.

Structure	FRET (EC_{50})
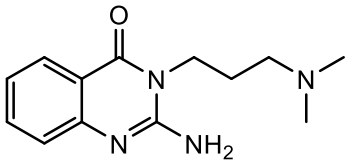 **8**	n.a.
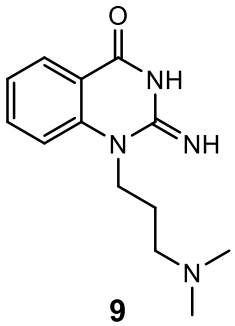 **9**	770 ± 190 µM
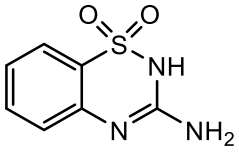 **11**	47 ± 30 µM
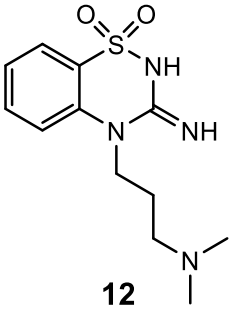 **12**	11 ± 7 µM

The guanine-like compounds **8** and **9** did not show significantly increased binding affinity with the N^1,N^1-dimethylpropyl-diamine side chain. **8** was essentially inactive in the FRET, and **9** was a weak binder comparable to the original 2-aminoquinazolinone from which it was derived from, with an EC_{50} of around 770 ± 190 µM. The benzothiadiazines **11** and **12** , however, proved to be highly active in the FRET assay, at an EC_{50} of 47 ± 30 µM for **11**, and EC_{50} of 11 ± 7 µM for **12**. This was a significant finding, as the benzimidazoles, benzoxazoles, and quinazolinones were all planar compounds, while the benzothiadiazine scaffold is not (**Figure 2.1.3**).

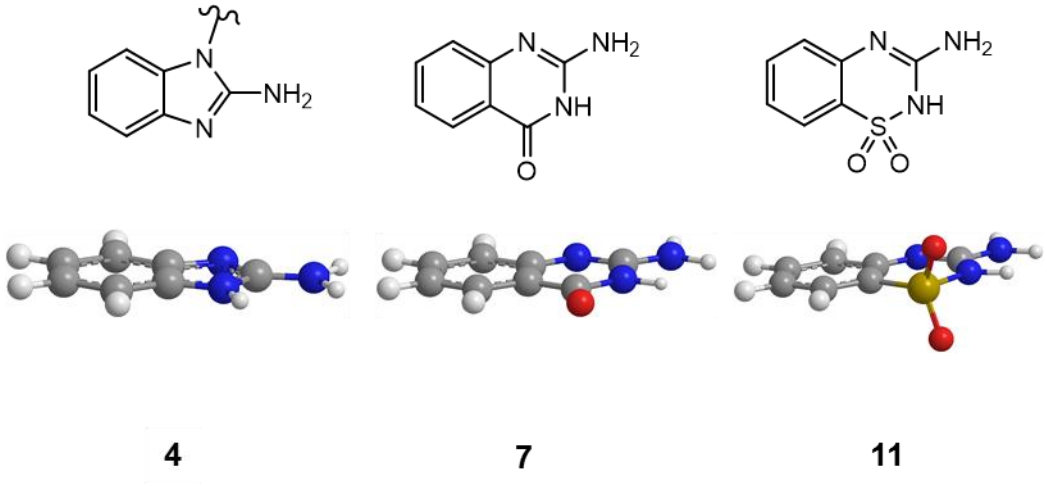

Figure 2.1.3: The predicted 3D structures of compounds **7** and **11** against the core of compound **2**. The SO_2 group of the benzothiadiazines like **11** shows a large difference in planarity breaking above and below the plane of the compound when compared to the previously discovered IRES inhibitors. Structures generated with chem3D and are in agreement with crystal structures of these scaffolds. [Hermann Lab, unpublished]

The SO_2 group projects above and below the plane of the compound which suggests that the IRES subdomain IIa ligand binding pocket can

accommodate nonplanar groups. Ongoing efforts in our lab are directed at derivatizing the benzothiadiazine scaffold to determine if improved affinity can be achieved. With the principle of breaking the planarity, knowing the binding pocket can accommodate larger non-planar groups, while keeping the guanidine-like moiety to allow hydrogen bonding to the Hoogsteen edge of the G110-C58 base pair in the binding pocket, I sought to design two new scaffolds to prepare ligands for the subdomain IIa target.

2.1.1 Design of novel benzodiazepinones to target HCV IRES subdomain IIa

The first design for a new scaffold was to make a 7-membered relative to the quinazolinone (**Figure 2.1.1.1**), compounds **13** and **14**.

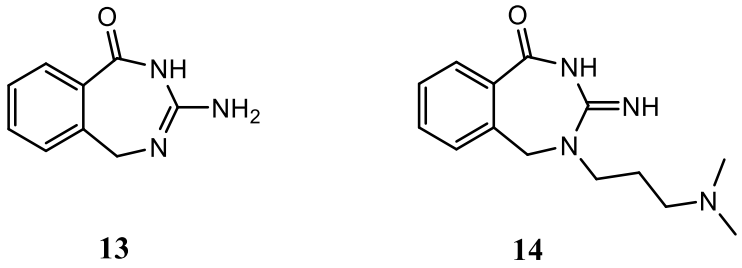

13 **14**

Figure 2.1.1.1: Design for compounds 3-amino-2,5-dihydro-1H-benzo[*e*][1,3]diazepin-1-one **13** and 4-(3-(dimethylamino)propyl)-3-imino-2,3,4,5-tetrahydro-1H-benzo[*e*][1,3]diazepin-1-one **14**.

Since the guanine bound at a FRET EC_{50} of about 1 mM, and the larger space filling quinazolinone had double the affinity at an EC_{50} of about 500 µM, I wanted to increase the size of the ring again while keeping the benzene pie stacking interactions intact. However, because of the success of the

benzothiadiazines, the 7-memebered ring would be useful two-fold in also greatly breaking planarity compared to the quinazolinones and hopefully filling the IRES binding pocket better. Depicted in (**Figure 2.1.1.2**) is a 3D model of the 7-membered benzodiazopinone **13** compared to the quinazolinone **7** and benzothiadiazine compound **11** to show the difference in planarity compared to the quinazolinone and compare it to the highly active, non-planar benzothiadiazine.

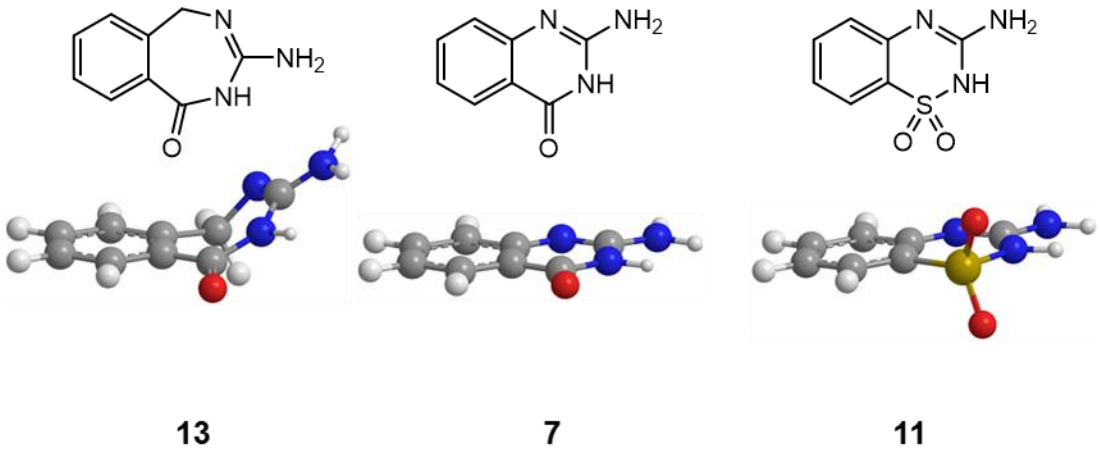

Figure 2.1.1.2: The predicted 3D structures of compounds **13**, **7**, and **11**. Structures generated with chem3D.

Since there is no standard way to make a 7-membered ring, but several current effective drugs on the market that include these benzodiazepinones such as Valium, I knew it would be both a challenging and rewarding experience to synthesize this scaffold.

2.1.2 Design of spirocyclopropane derivatives targeting HCV IRES subdomain IIa

The second scaffold designed was a dimethyl and cyclopropyl-quinazolin-amine (**Figure 2.1.2.1**), compounds **15**, **16**, and **17**, which were designed as a direct mimic of the shape of the highly effective benzothiadiazines sulfoxide group, to see if the compound could fill the binding pocket of the IRES better than the benzothiadiazine in terms of physical space, or if the hydrogen bonding of the benzothiadiazine was an advantage and see if this scaffold could compete in FRET activity.

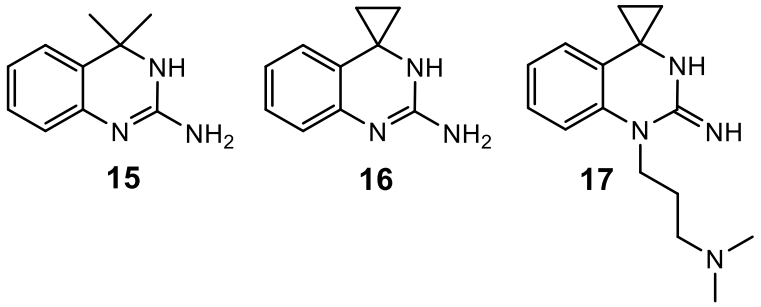

Figure 2.1.2.1: The scaffolds designed to mimic the shape of the benzothiadiazines sulfonyl group. 4,4-dimethyl-3,4-dihydroquinazolin-2-amine **15**, 3'H-spiro[cyclopropane-1,4'-quinazolin]-2'-amine **16**, and 3-(2'-imino-2',3'-dihydro-1'H-spiro[cyclopropane-1,4'-quinazolin]-1'-yl)-N,N-dimethylpropan-1-amine **17**.

The dimethyl-quinazolin-amine version **15** was explored, but the dimethyl compound holding a bond angle between its two out stretched methyl groups has the tetrahedral sp^3 hybridized angle of 109.5°, whereas the cyclopropyl compound has a tighter angle between its out of plane carbons of about 60° due to its unique hybridization from ring strain and forming a tight triangle. While also

having two less hydrogens overall than the dimethyl, the cyclopropyl was expected to fit into the binding pocket of the IRES better than the dimethyl version (**Figure 2.1.2.2**).

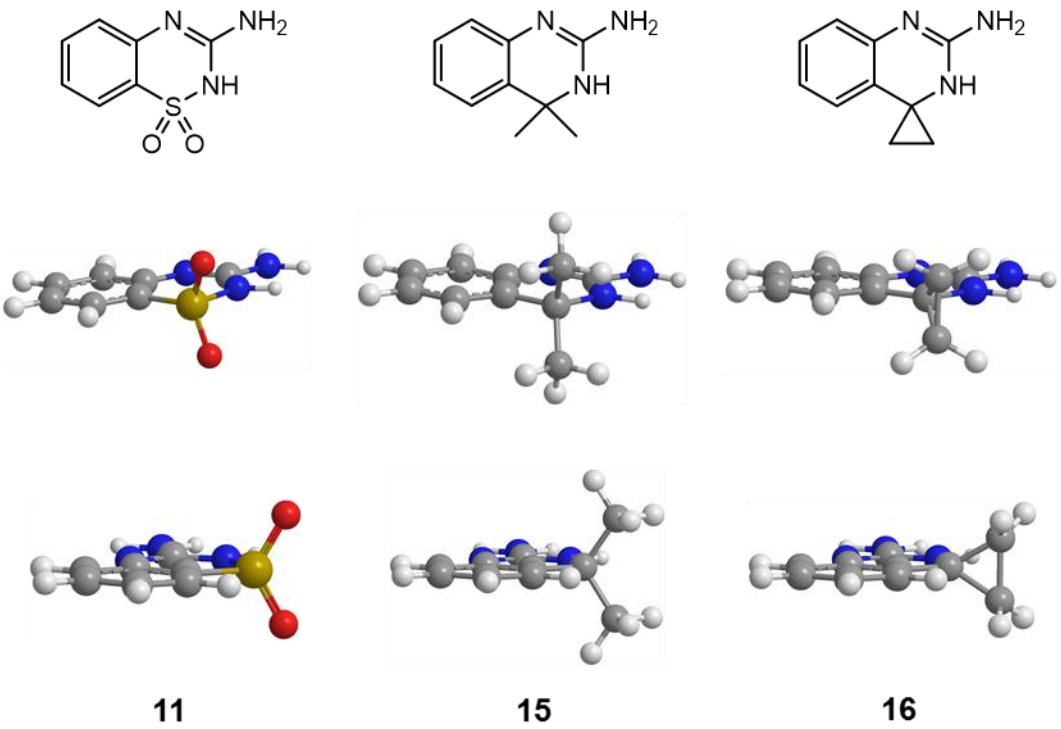

Figure 2.1.2.2: The predicted 3D structures of **11**, **15**, and **16**. Structures generated via chem3D, chem3D generated structure for benzothiadiazine **11** is in agreement with the small molecule structure. [Hermann Lab, unpublished]

The traditional way cyclopropyl rings are made is to have a carbene attack a double bond, but a recent publication showed a more accessible approach using a Grignard and a Nitrile in a Szymoniak variation of the Kulinkovich reaction (**Figure 2.1.2.3**).

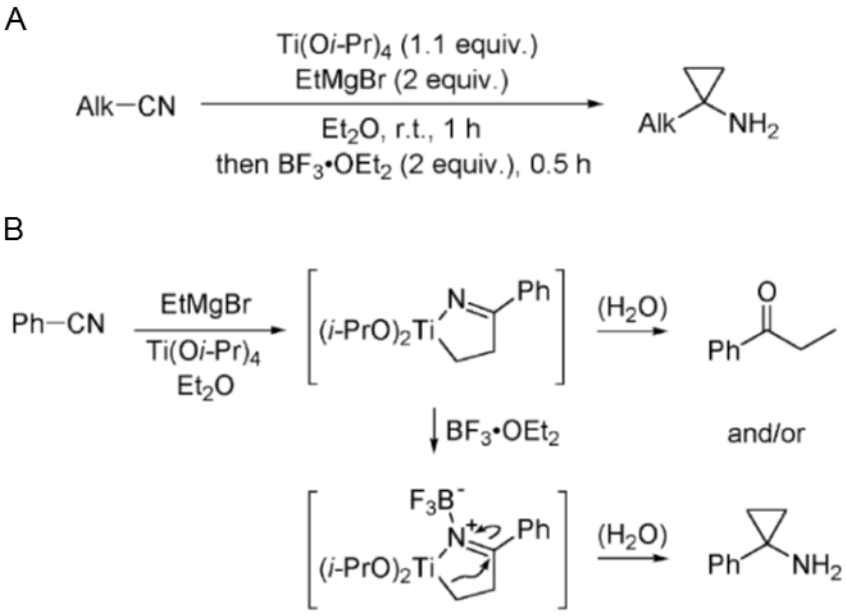

Figure 2.1.2.3: The synthesis of cyclopropylamines from nitriles, a Szymoniak variation of the Kulinkovich reaction. A) The general reaction scheme. B) The hypothesized overview of the reaction, the Titanium catalyst couples nitrile and ethyl Grignard together, and only yields cyclopropylamine product when Lewis acid is used to facilitate the cyclopropyl ring formation upon aqueous workup. Figure modified from ref[37], 2003, American Chemical Society.

With reasonable access to the cyclopropyl moiety I knew this scaffold could be unique and interesting to synthesize and test in the HCV IRES FRET assay.

2.2 Benzodiazepinones as new ligands for targeting HCV IRES subdomain IIa

2.2.1 Synthesis of benzodiazepinones 13 and 14

The synthesis of the 7-membered diazepinones **13** and **14** was originally envisioned to be synthesized similar to the quinazolinone **9** in a one pot, two

step reaction, with intramolecular nucleophilic substitution of the methyl ester after nucleophilic substitution of the benzyl amine on compound **18** to previously synthesized compound **10** (**Scheme 2.2.1.1**).

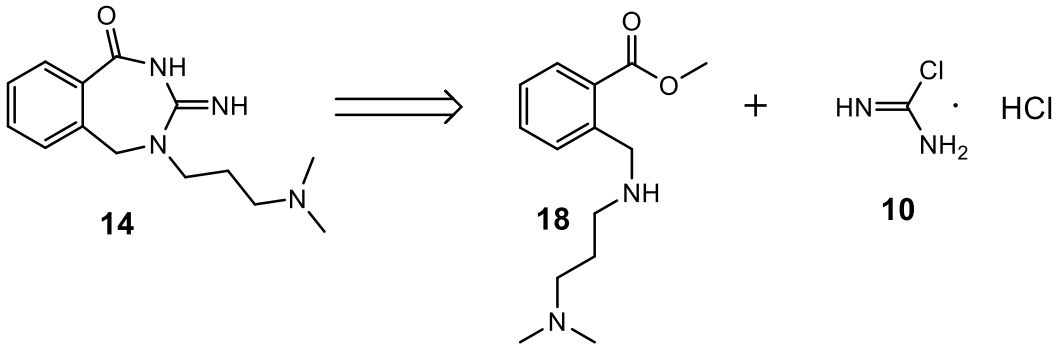

Scheme 2.2.1.1: Retrosynthetic analysis of benzodiazepinone **14**.

This precursor **18** would be synthesized via nucleophilic substitution with the desired commercially available amine, in this case N^1,N^1-dimethylpropyl-diamine or 3-(dimethylamino)-1-propylamine, with commercially available methyl 2-(chloromethyl)benzoate. While **18** was synthesized in nearly quantitative yields, attempts to make **14** failed due to the rapid intramolecular cyclization to the 5-membered ring with the amine and methyl ester giving the unwanted side product **19** (**Scheme 2.2.1.2**).

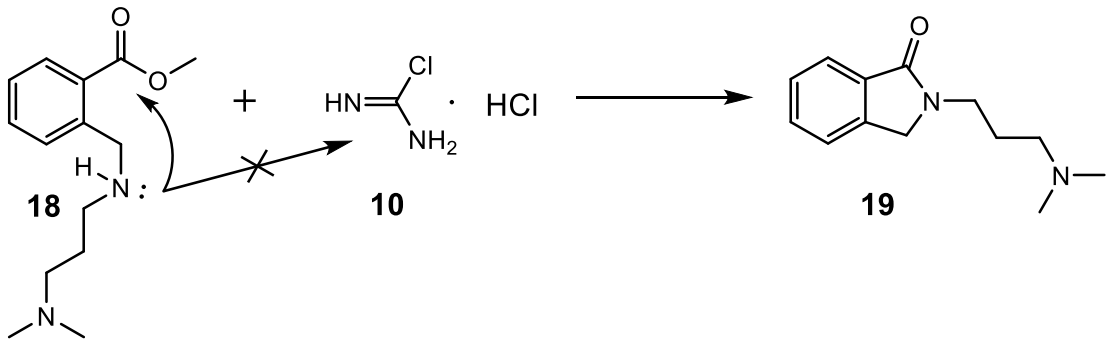

Scheme 2.2.1.2: Synthetic depiction of the reaction involving methyl ester **18** and **10** giving unwanted intramolecular side product **19**.

With the inability to prepare the diazepinone **14** due to the unwanted 5-membered intramolecular cyclization, a modification to the synthetic route was required. Since the benzyl amine preferred substitution at the methyl ester for the 5-membered ring over attack of the electrophilic compound **10** after several attempts, it was clear the guanidine-like moiety would need to be installed before adding it to the ring, and ensure that the benzyl nitrogen could not be nucleophilic (**Figure 2.2.1.1**).

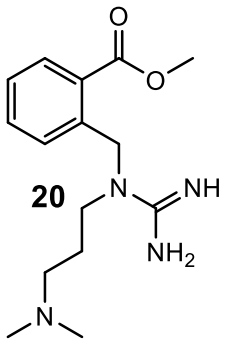

Figure 2.2.1.1: Methyl 2-((1-(3-(dimethylamino)propyl)guanidino)methyl) benzoate **20**.

As the benzyl nitrogen would be fully substituted, it could not form the 5-membered intramolecular ring to compound **19** it had previously made. This guanidino-methyl benzoate **20** would be synthesized via nucleophilic substitution of the same commercially available methyl 2-(chloromethyl)benzoate previously used with a di-Boc protected substituted guanidine **21** to form the methyl ester **22**. Deprotection of **22** via Trifluoroacetic acid (TFA) or hydrochloric acid (HCl) would afford the desired unprotected methyl ester **20** (**Scheme 2.2.1.3**).

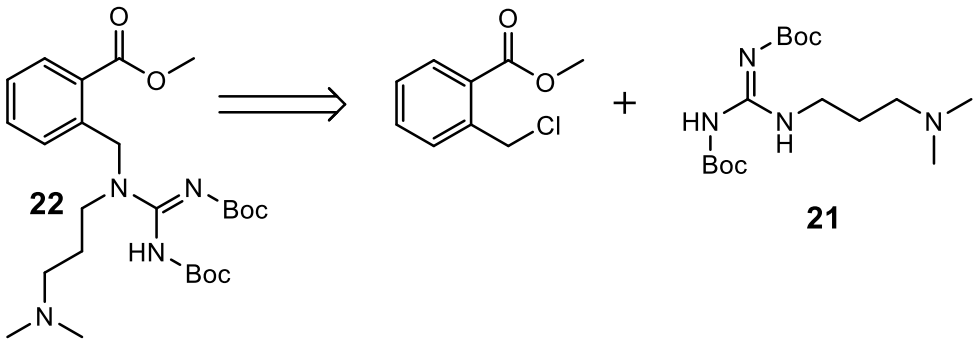

Scheme 2.2.1.3: Retrosynthetic analysis of Boc protected methyl ester **22**.

(*Z*)-1-(3-(dimethylamino)propyl)-2,3-bis(*tert*-butoxycarbonyl) guanidine **21** would be synthesized via nucleophilic substitution of commercially available 1*H*-pyrazole-1-carboximidamide and commercially available amine 3-(dimethylamino)-1-propylamine (**Scheme 2.2.1.4**).[38]

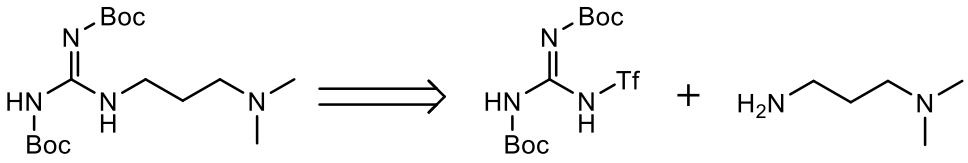

21

Scheme 2.2.1.4: Retrosynthetic analysis of Boc protected substituted guanidine **21**.

While synthesis of **22** was readily accomplished in good yields, and deprotection with TFA afforded the unprotected methyl ester **20**, attempts to cyclize **20** into the final compound **14** were unsuccessful. The 7-membered ring not being nearly as favorable as the 5 or 6 membered variants and the methyl ester being one of the less electrophilic carbonyls likely reasons as to why this cyclization did not occur. The main products were unreacted starting materials and degraded unidentifiable side products when higher temperatures were used. This in mind, the carbonyl was targeted to change and use a more electrophilic derivative in the synthetic route to see if altercations could be made to aid the final 7-membered ring cyclization step. The revised synthesis involved attempts to make the acid chloride **23** for the final cyclization step as the strength of the acid chloride as an electrophile should allow the 7-membered ring to be formed. The synthesis would begin with the formation of the methyl ester **22** exactly as before with the substituted and protected guanidine **21** undergoing nucleophilic substitution with commercially available methyl 2-(chloromethyl)benzoate (**Scheme 2.2.1.3**). Aqueous hydrolysis would afford the benzoic acid **24**. Conversion to the acyl chloride **25** would be afforded via oxalyl

chloride and catalytic DMF. Finally, deprotection of the Boc groups with dry TFA or HCl would afford the acyl chloride **23** which would immediately undergo cyclization in a nucleophilic substitution of the acid chloride to close the 7-membered ring to compound **14** (**Scheme 2.2.1.5**).

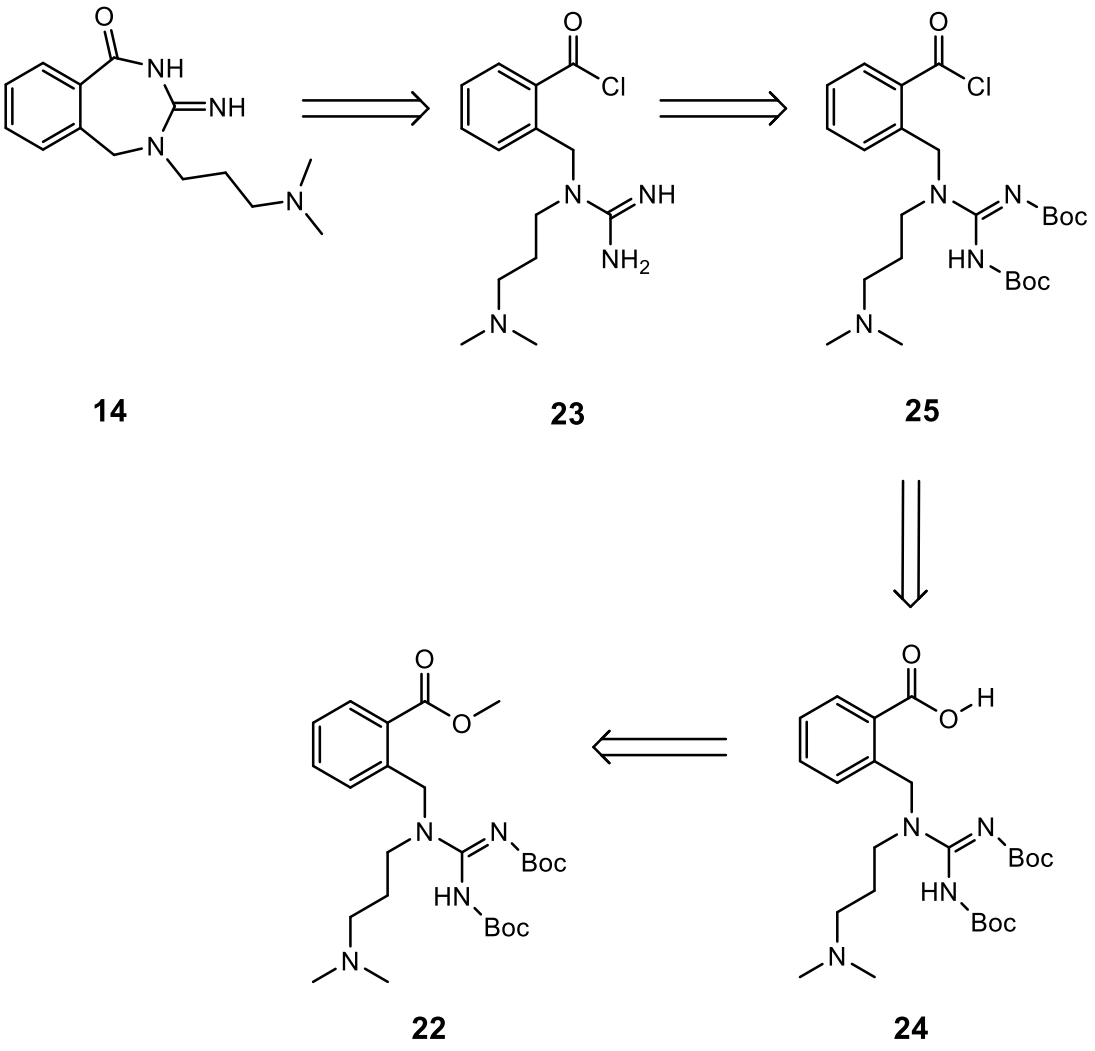

Scheme 2.2.1.5: Retrosynthetic analysis of substituted benzodiazepinone **14**.

The conversion of methyl ester **22** to benzoic acid **24** was not achieved however. It was done under basic conditions to avoid Boc deprotection, but a

majority of the Boc protection groups appeared to come off in the hydrolysis and the guanidine moiety needed to be protected in order for conversion of the acid **24** to the acid chloride **25** to convert smoothly. A change in the synthetic route was made to attempt using commercially available 2-(bromomethyl)benzoic acid with compound **21** to afford the benzoic acid **24** without the need of aqueous hydrolysis. This would then be converted to the acid chloride **22** in the same fashion via oxalyl chloride and catalytic DMF. However, this did not succeed as there was no evidence of nucleophilic substitution of guanidine **21** to the commercially available 2-(bromomethyl)benzoic acid, simply both starting materials could be observed until heat caused the degradation of the guanidine **21**.

As the cyclization step of the 7-membered ring to the carbonyl carbon was becoming exhausted, the synthetic route was revised to first make the nucleophilic substitution at the carbonyl carbon first, then attempt to cyclize at the ortho benzyl carbon to close the ring. Nucleophilic substitution of guanidine to commercially available 2-(chloromethyl)benzoyl chloride could allow a one-pot, two step reaction in which nucleophilic substitution at the acid chloride would take place, followed by intramolecular S_N2 nucleophilic substitution of the benzyl chlorine to close the 7-membered ring and afford compound **13** (**Scheme 2.2.1.6**).

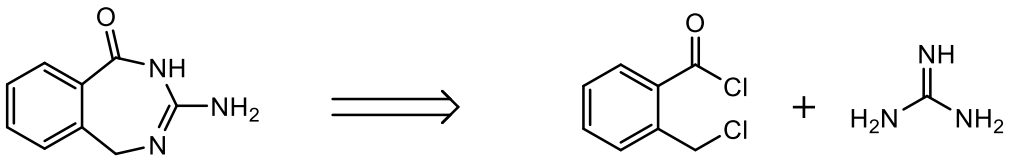

13

Scheme 2.2.1.6: Retrosynthetic analysis of benzodiazepinone **13**.

A similar reaction was envisioned and designed for compound **14**, which would involve the same nucleophilic substitution of a substituted guanidine **26** to commercially available 2-(chloromethyl)benzoyl chloride for a one-pot, two step reaction in which nucleophilic substitution at the acid chloride would take place, followed by intramolecular S_N2 nucleophilic substitution of the benzyl chlorine to close the 7-membered ring and afford compound **14**. (**Scheme 2.2.1.7**)

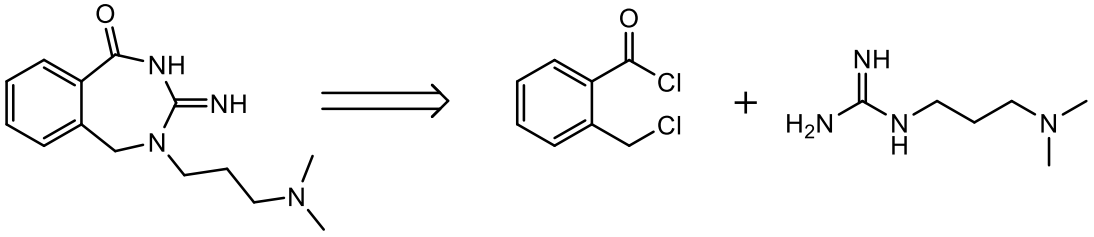

14 **26**

Scheme 2.2.1.7: Retrosynthetic analysis of substituted benzodiazepinone **14**.

The regioselectivity of the sidechain was desired at the position shown in compound **14**. This could be achieved with this synthesis since the nucleophilic substitution to the acid chloride is so fast, it is kinetically driven, and the two unsubstituted amines in **26** should react quicker than the sterically

hindered secondary amine. Finally, the intramolecular S_N2 nucleophilic substitution of the benzyl chlorine would be a relatively slow reaction rate if brought from cooler temperatures and therefore more thermodynamically driven, which means the more nucleophilic secondary amine should be favored to close the 7-membered ring and give the desired regio-isomer of **14**. The substituted guanidine **26** would be synthesized via nucleophilic substitution with commercially available 3-(dimethylamino)-1-propylamine and commercially available 1H-pyrazole-1-carboximidamide. (**Scheme 2.2.1.8**).[38]

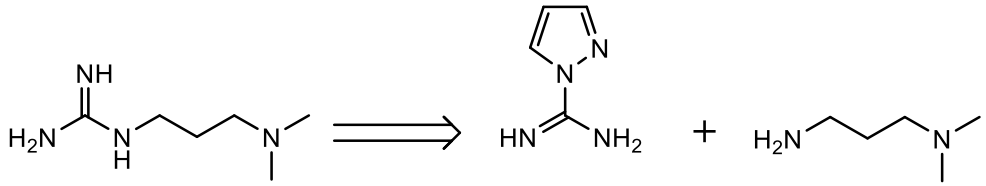

26

Scheme 2.2.1.8: Retrosynthetic analysis of substituted guanidine **26**.

The benzodiazepinone **13** 3-amino-2,5-dihydro-1H-benzo[*e*][1,3]diazepin-1-one was readily prepared in a one-pot synthesis from commercially available 2-(chloromethyl)benzoyl chloride and guanidine hydrochloride (**Scheme 2.2.1.9**). The reaction was cooled to 0°C with an ice bath to avoid early nucleophilic substitution at the benzyl chloride. It is critical to add 2-(chloromethyl)benzoyl chloride slowly to the guanidine as the reverse order yielded no product due to possible double and triple nucleophilic substitutions from the guanidine to 2-(chloromethyl)benzoyl chloride.

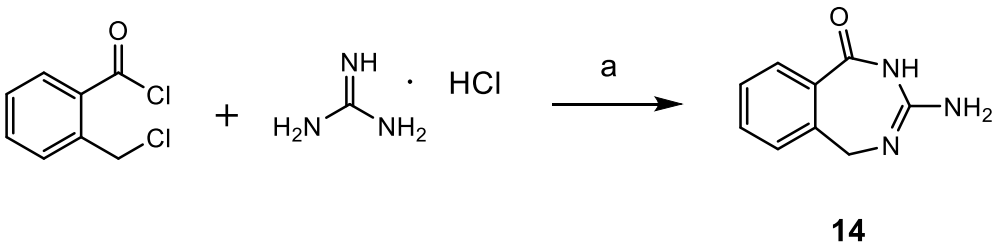

14

Scheme 2.2.1.9: Synthesis of benzodiazepinone **14**.

Reagents and conditions: a) K_2CO_3, THF, 0°C to R.T. over 4 hours, 33%.

The synthesis of the substituted guanidine **26** was accomplished via nucleophilic substitution of commercially available3-(dimethylamino)-1-propylamine and 1H-pyrazole-1-carboximidamide (**Scheme 2.2.1.10**).[38]

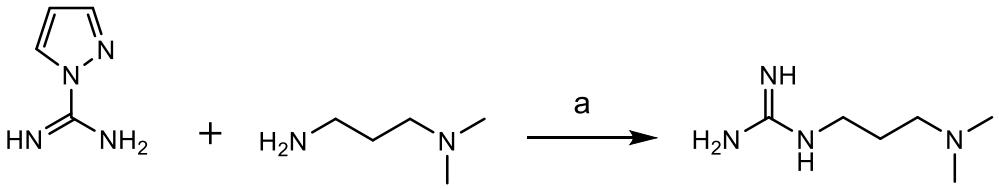

26

Scheme 2.2.1.10: Synthesis of substituted guanidine **26**.

Reagents and conditions: a) K_2CO_3, DMF, 70°C, 90%.

The substituted benzodiazepinone **14** 4-(3-(dimethylamino)propyl)-3-imino-2,3,4,5-tetrahydro-1H-benzo[*e*][1,3]diazepin-1-one was synthesized in the same manner as **13**, in a one-pot synthesis from commercially available 2-(chloromethyl)benzoyl chloride and the substituted guanidine **26** (**Scheme 2.2.1.11**). The reaction was cooled to 0°C with an ice bath to avoid early nucleophilic substitution at the benzyl chloride, and promote the secondary amine in compound **26** to close the ring via S_N2 nucleophilic substitution more

favorably over the remaining primary amine when brought slowly back up to room temperature. Again it is critical to add 2-(chloromethyl)benzoyl chloride slowly to the substituted guanidine **26** as the reverse order yields no product.

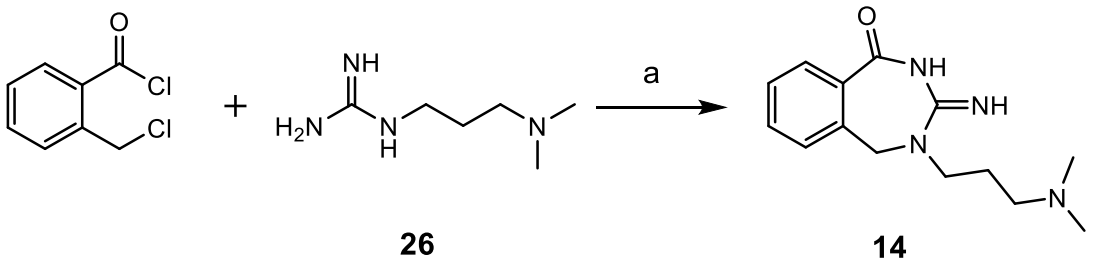

26 **14**

Scheme 2.2.1.11: Synthesis of substituted benzodiazepinone **14**.

Reagents and conditions: a) K_2CO_3, THF, 0°C to R.T. over 4 hours, 29%.

The two benzodiazepinones **13** and **14** required HPLC reverse-phase purification and the product for both was identified via evaporative light scattering detector (ELSD) and mass spectrometry (MS) analysis. While it appeared both compounds were clean and homogenous after HPLC, the NMR analysis yielded unexpected results. It initially appeared as though there were two compounds for both benzodiazepinones **13** and **14** as two sets of the four benzene peaks and two sets of the benzyl ethyl singlet peaks could be seen, with matching relative integrations (**Figure 2.2.1.2**).

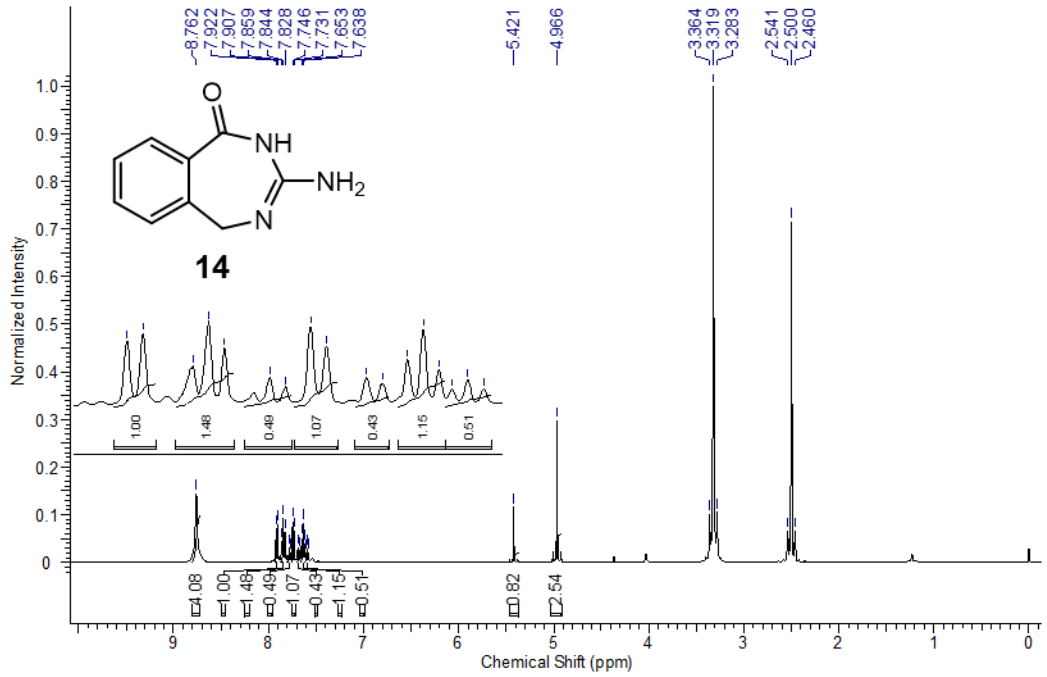

Figure 2.2.1.2: The ^{1}H NMR spectra of benzodiazepinone **13** at 500MHz, in DMSO-*d*$_6$. An expanded section of the benzene protons is shown which highlights the two sets of peaks with relative integration differences to be ~1:0.4.

Despite both compounds showing two sets of proton and carbon peaks in the NMR spectra, high-resolution mass spectrometry data (HRMS) and the ELSD signal recorded during reverse-phase HPLC purification suggested that the compounds were isolated as a mixture of tautomers (**Figure 2.2.1.3**).

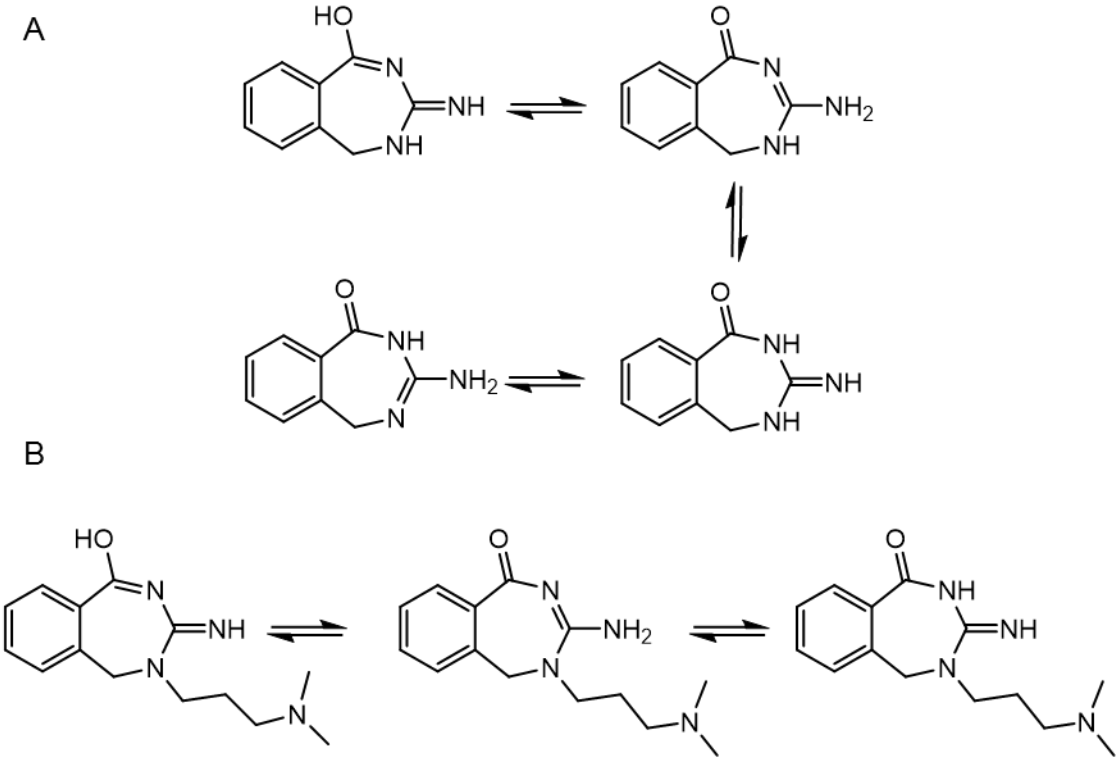

Figure 2.2.1.3: Tautomerization and resonance of the benzodiazepinones **13** (A) and **14** (B).

This would validate the change in benzene peaks that is observed in the NMR spectra as the keto form would shift benzene peaks downfield where the enol form would shift them upfield. It is in agreement with similar compounds N-methylbenzamide and 1-methoxy-N-methyl-1-phenylmethanamine, which represent keto and enol tautomeric forms, which show shifts in proton and carbon NMR peaks compared to each other similar to that seen in the benzodiazepinones **13** and **14**.[39],[40] Where typically the keto form is favored over the enol form, it appears the 7-membered ring helps to shift the equilibrium to a ratio close to 2.5:1 for **13**, and 1:1 for **14** based on proton integrations. More evidence for tautomerization is seen in the NMR spectrum for **14**, where a single

set of signals is observed for the alkyl side chain which would be mostly unaffected by the tautomerism (some broadening occurred), and the integration of benzene peaks relative to the alkyl side chain is affected by the ratio of tautomers, as would be expected. (**Figure 2.2.1.4**).

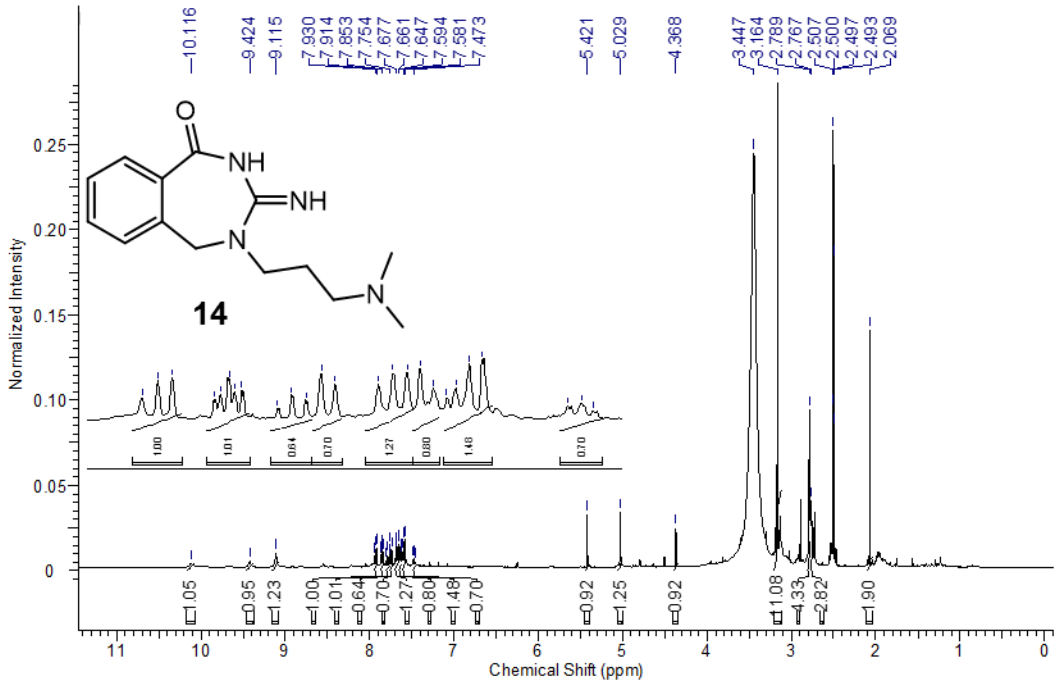

Figure 2.2.1.4: The ^{1}H NMR spectra of benzodiazepinone **14** at 500MHz, in DMSO-d_6. An expanded section of the benzene protons is shown which highlights the two sets of peaks with relative integration differences to be ~1:1.

With the compounds clean of impurities but unable to separate the tautomers from each other, the mixture was tested in the FRET assay.

2.2.2 Testing of benzodiazepinones 13 and 14 as ligands targeting HCV IRES subdomain IIa

The synthesized benzodiazepinones **13** and **14** were tested in the FRET assay to determine if they would bind to the subdomain IIa of the HCV IRES construct. Although they did show some competence in binding to the IRES, the affinity was weak (**Table 2.2.2.1**). Like some of the guanidine counterparts, the benzodiazepinones caused the signals of the Cy3, Cy5, and FRET to go down with increasing concentrations. This could suggest possible non-specific interactions that cause RNA to precipitate which makes calculating the EC_{50} difficult. However, the Cy3 signal went down less compared to the FRET and Cy5 signals, suggesting some binding to the IRES.

Table 2.2.2.1: Ligand affinity of **13** and **14** measured by FRET assay. EC_{50} is the concentration required for a fifty percent reduction in the observed FRET signal.

Structure	FRET (EC_{50})
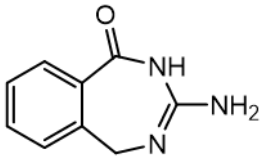 **13**	653 ± 126 µM
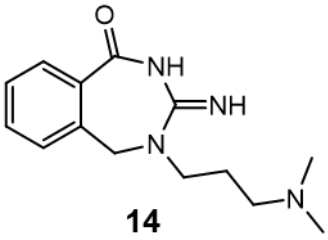 **14**	> 1500 µM

The benzodiazepinones **13** and **14** showed binding to the HCV IRES construct, but without meaningful affinity improvement over other guanine-like compounds. A main drawback of the 7-membered ring scaffold may be the occurrence of possible tautomers among which some may not bind to the IRES RNA. If this is the case, then the concentration of the active isomer is diluted by other tautomeric forms. The 7-memebered ring could also be too non-planar and reduce binding to the IRES pocket due to the bulkiness of the large ring. Its low binding affinity, tautomeric properties, and inability to isolate a single active isomer make the 7-membered benzodiazepinones scaffold a less desirable choice to be further optimized for the IRES.

2.2.3 Materials and Methods

3-amino-2,5-dihydro-1H-benzo[*e*][1,3]diazepin-1-one (13)

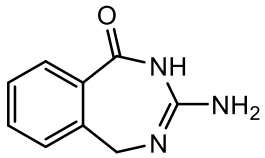

13

Figure 2.2.3.1: 3-amino-2,5-dihydro-1H-benzo[*e*][1,3]diazepin-1-one (**13**).

A solution of Guanidine Hydrochloride (2.995 mmol, 0.286 g) and Potassium Carbonate (6.011 mmol, 0.831 g) in 40mL of THF under argon was prepared and cooled to 0°C with an ice bath with magnetic stirring. 2-(chloromethyl)benzoyl chloride (1.986 mmol, 0.285 mL) was added dropwise with a syringe. This was allowed to come to room temperature from ambient atmospheric temperature overnight. After 12 hours, the solution was filtered and rinsed with MeOH (25 mL), and the solvent was removed *in vacuo* to yield a yellow oil. This was purified using reverse-phase HPLC in multiple runs at a gradient of 0.2%-25% acetonitrile in water to give **13** as a white solid in a purified yield of 33%.

13: ^{1}H NMR (500 MHz, DMSO-d_6) δ 8.762 (br s, 1H, NH_2), 7.915 (d, 1H, J = 7.5Hz), 7.844 (m, 1H), 7.785 (t, 1H, J = 7.5Hz), 7.739 (d, 1H, J = 7.5 Hz), 7.685 (d, 1H, J = 7.5 Hz), 7.638 (t, 1H, J = 8 Hz), 7.595 (t, 1H, J = 8 Hz), 5.421 (s, 2H),

4.966 (s, 2H); ^{13}C NMR (500 MHz, DMSO-d_6) δ 169.797, 154.704, 147.787, 147.113, 141.806, 135.538, 134.651, 129.488, 129.392, 129.266, 125.332, 125.047, 124.318, 123.418, 70.347, 49.865; HRMS mass calculated $C_9H_{10}N_3O$ $[M+H]^+$ = 176.0818, found 176.0815; Delta -1.7 ppm.

1-(3-(dimethylamino)propyl)guanidine (26)

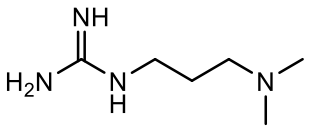

26

Figure 2.2.3.2: 1-(3-(dimethylamino)propyl)guanidine (**26**).

To a solution of 1H-pyrazole-1-carboximidamide hydrochloride (6.788 mmol, 0.994 g) and Potassium Carbonate (9.122 mmol, 1.260 g) in 5 mL of DMF, 3-(dimethylamino)-1-propylamine (4.511 mmol, 0.569 mL) was added. The reaction mixture was flushed with argon, stirred magnetically, and heated to 60°C for 8 hours. The solvent was removed *in vacuo* to yield a yellow oil. This was used without further purification to the next step. However, for analytical measurements, reverse-phase HPLC at a gradient of 0.2%-25% acetonitrile in water gave **26** as a colorless oil at 90% yield.[38]

26: ^{1}H NMR (500 MHz, DMSO-d_6) δ 9.689 (br s, 1H, NH), 7.858 (br s, 1H, NH), 3.143 (q, 2H, J = 6 Hz), 3.024 (m, 2H), 2.766 (s, 6H), 1.809 (p, 2H, J = 8 Hz); ^{13}C NMR (500 MHz, DMSO-d_6) δ 157.188, 54.569, 42.744, 38.340, 24.120;

HRMS mass calculated $C_6H_{17}N_4$ $[M+H]^+$ = 145.1448, found 145.1446; Delta -1.4 ppm.

4-(3-(dimethylamino)propyl)-3-imino-2,3,4,5-tetrahydro-1H-benzo[*e*][1,3]diazepin-1-one (14)

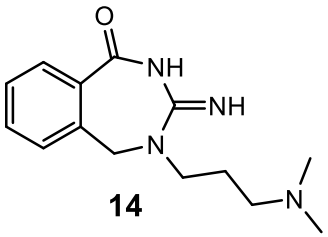

14

Figure 2.2.3.3: 4-(3-(dimethylamino)propyl)-3-imino-2,3,4,5-tetrahydro-1H-benzo[*e*][1,3]diazepin-1-one (**14**).

A solution of 1-(3 (dimethylamino)propyl)guanidine (2.950 mmol, 0.425 g) and Potassium Carbonate (6.001 mmol, 0.829 g) in 40mL of THF under argon was prepared and cooled to 0°C with an ice bath with magnetic stirring. 2-(chloromethyl)benzoyl chloride (1.986 mmol, 0.285 mL) was added dropwise with a syringe. This was allowed to come to room temperature from ambient atmospheric temperature overnight. After 12 hours, the solution was filtered and rinsed with MeOH (25 mL), and the solvent was removed *in vacuo* to yield a yellow oil. This was purified using reverse-phase HPLC in multiple runs at a gradient of 0.2%-25% acetonitrile in water to give **14** as a yellow oil in a purified yield of 29%.

14: ^{1}H NMR (500 MHz, DMSO-d_6) δ 10.116 (br s, 1H, NH), 9.424 (br s, 1H, NH), 9.115 (br s, 1H, NH), 7.930 (t, 1H, J = 8.5 Hz), 7.853 (m, 1H), 7.786 (t, 1H, J = 7.5 Hz), 7.747 (d, 1H, J = 7.5 Hz), 7.677 (t, 1H, J = 8 Hz), 7.640 (d, 1H, J = 7 Hz), 7.594 (m, 1H), 7.473 (t, 1H, J = 6.5 Hz), 5.421 (s, 1H), 5.029 (s, 1H), 4.368 (s, 1H), 3.164 (s, 12H), 2.789 (m, 4H), 2.767 (m, 4H), 2.069 (m, 4H); ^{13}C NMR (500 MHz, DMSO-d_6) δ 173.010, 172.473, 170.997, 160.763, 160.511, 154.086, 148.460, 142.009, 136.565, 135.802, 133.160, 130.351, 129.159, 126.116, 125.850, 125.010, 124.151, 124.107, 71.476, 55.325, 49.858, 46.575, 43.640, 43.581, 35.575; HRMS mass calculated $C_{14}H_{21}N_4O$ $[M+H]^+$ = 261.1710, found 261.1708; Delta -0.8 ppm.

2.2.4 Spectral Data

Nuclear Magnetic Resonance

Spectrum 2.2.4.1: 3-amino-2,5-dihydro-1H-benzo[*e*][1,3]diazepin-1-one (**13**) ^{1}H NMR (500MHz, DMSO-d_6).

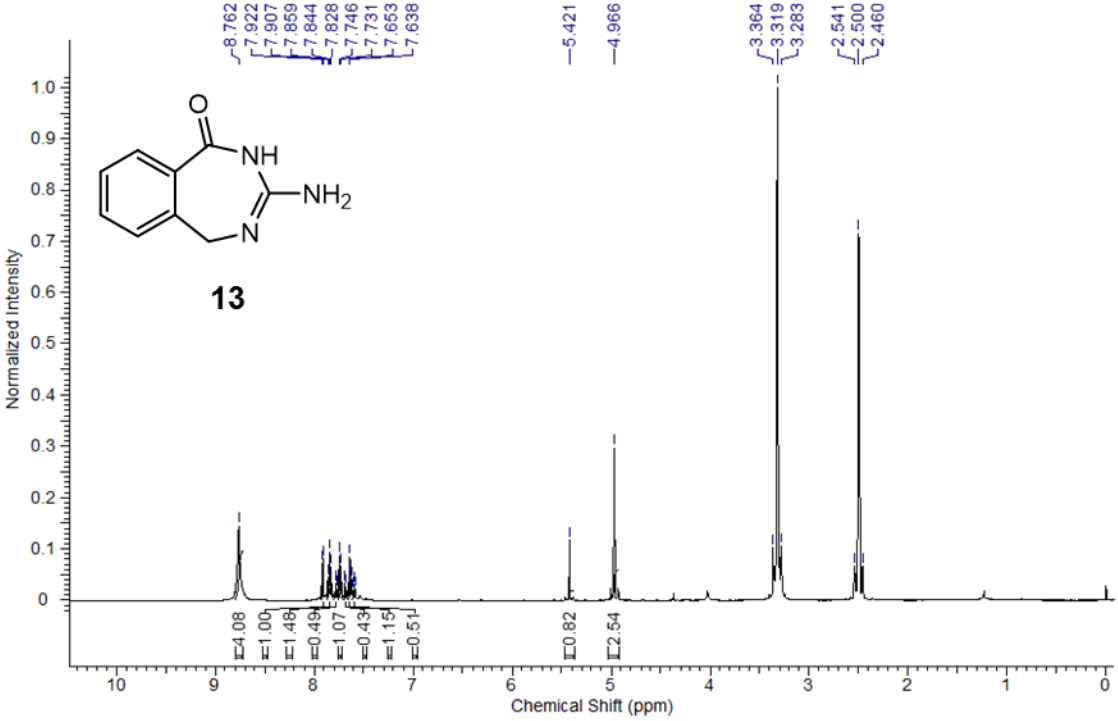

Spectrum 2.2.4.2: 3-amino-2,5-dihydro-1H-benzo[*e*][1,3]diazepin-1-one (**13**) ^{13}C NMR (500MHz, DMSO-d_6).

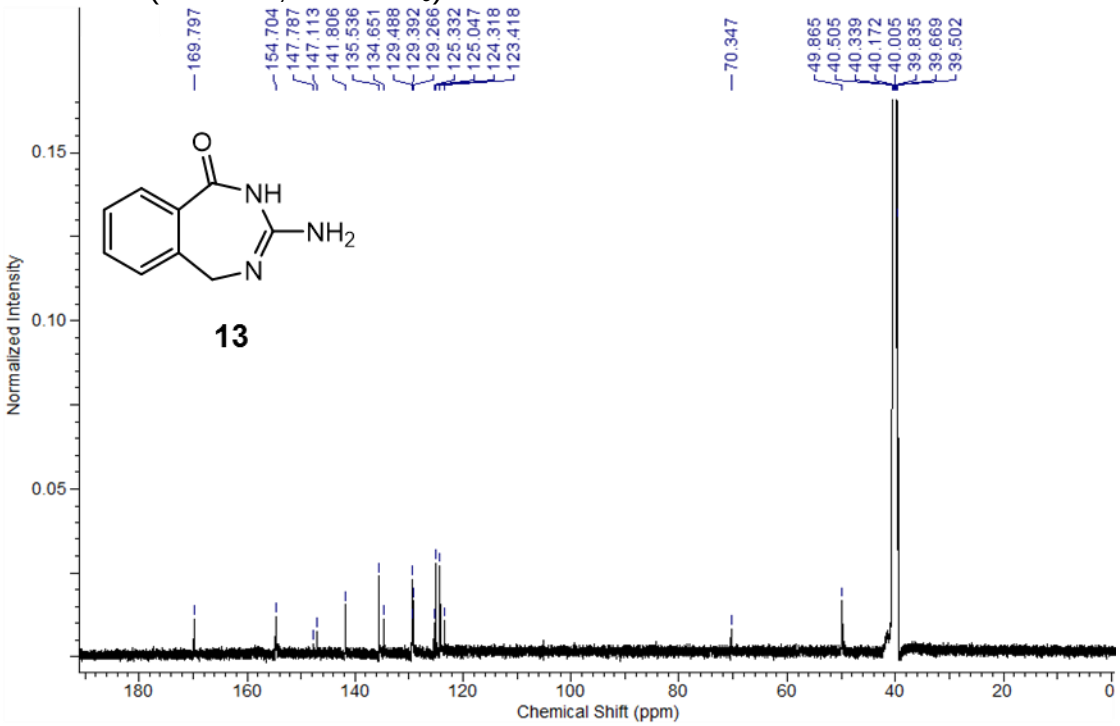

Spectrum 2.2.4.3: 1-(3-(dimethylamino)propyl)guanidine (**26**) ^{1}H NMR (500MHz, DMSO-d_6).

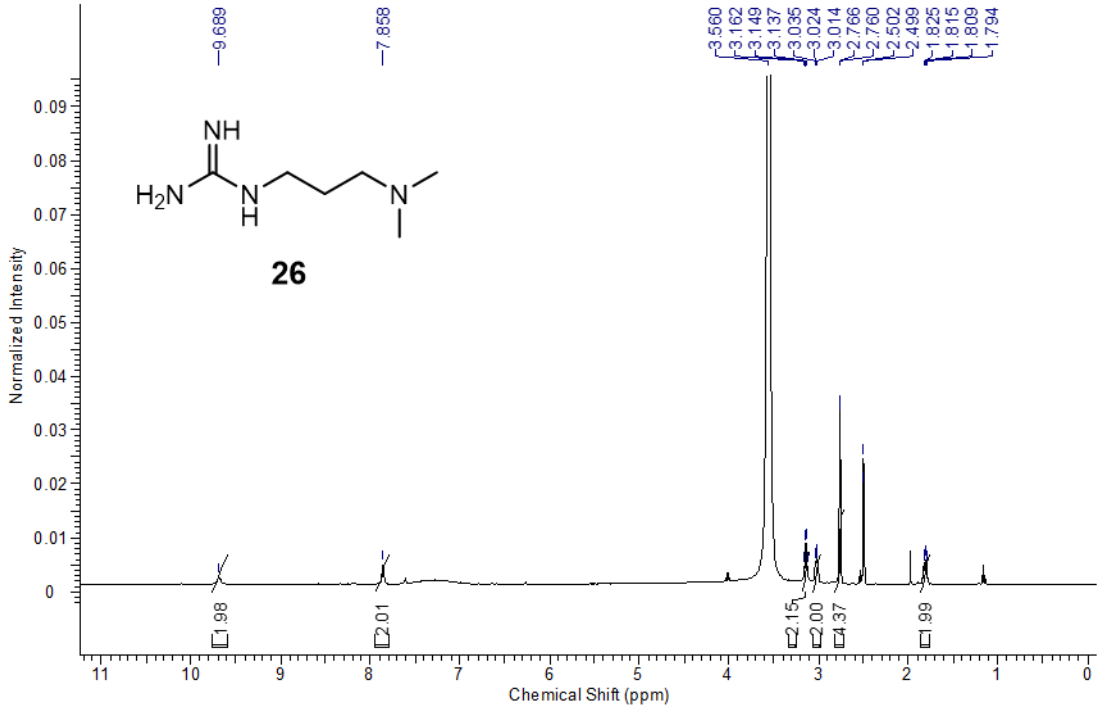

Spectrum 2.2.4.4: 1-(3-(dimethylamino)propyl)guanidine (**26**) ^{13}C NMR (500MHz, DMSO-d_6).

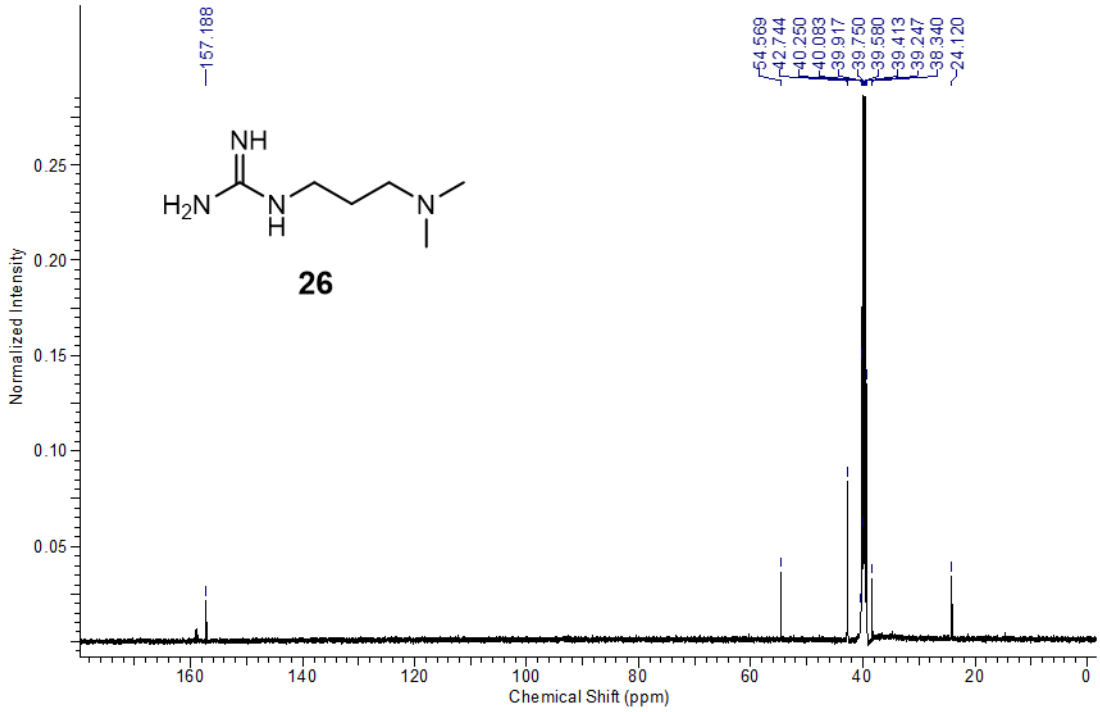

Spectrum 2.2.4.5: 4-(3-(dimethylamino)propyl)-3-imino-2,3,4,5-tetrahydro-1H-benzo[*e*][1,3]diazepin-1-one (**14**) ^{1}H NMR (500MHz, DMSO-d_6).

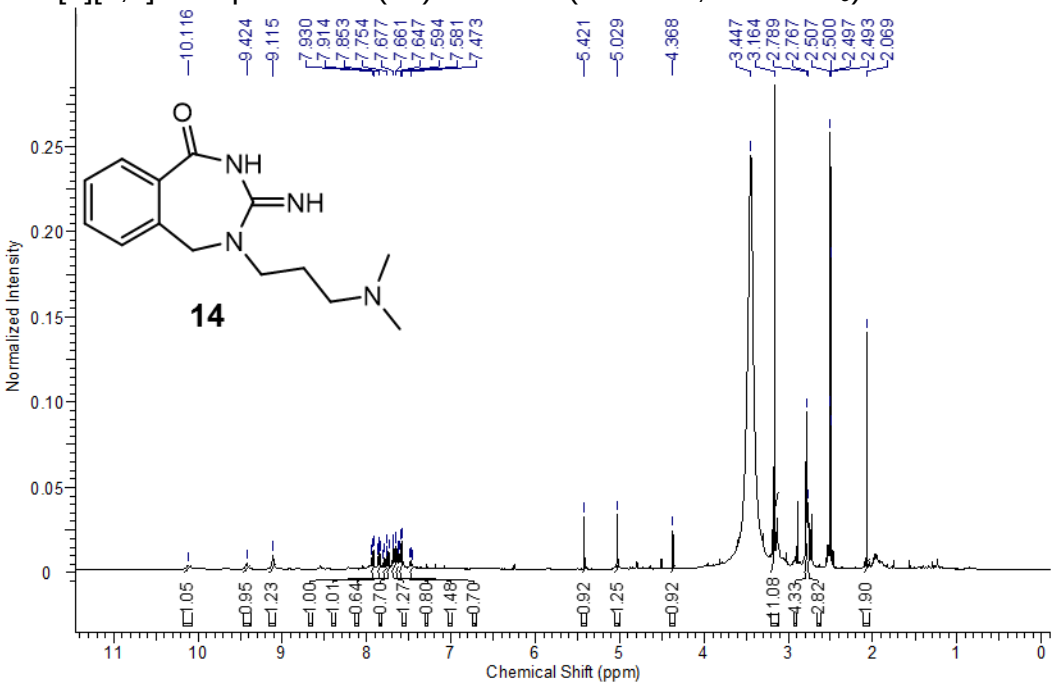

Spectrum 2.2.4.5: 4-(3-(dimethylamino)propyl)-3-imino-2,3,4,5-tetrahydro-1H-benzo[*e*][1,3]diazepin-1-one (**14**) ^{13}C NMR (500MHz, DMSO-d_6).

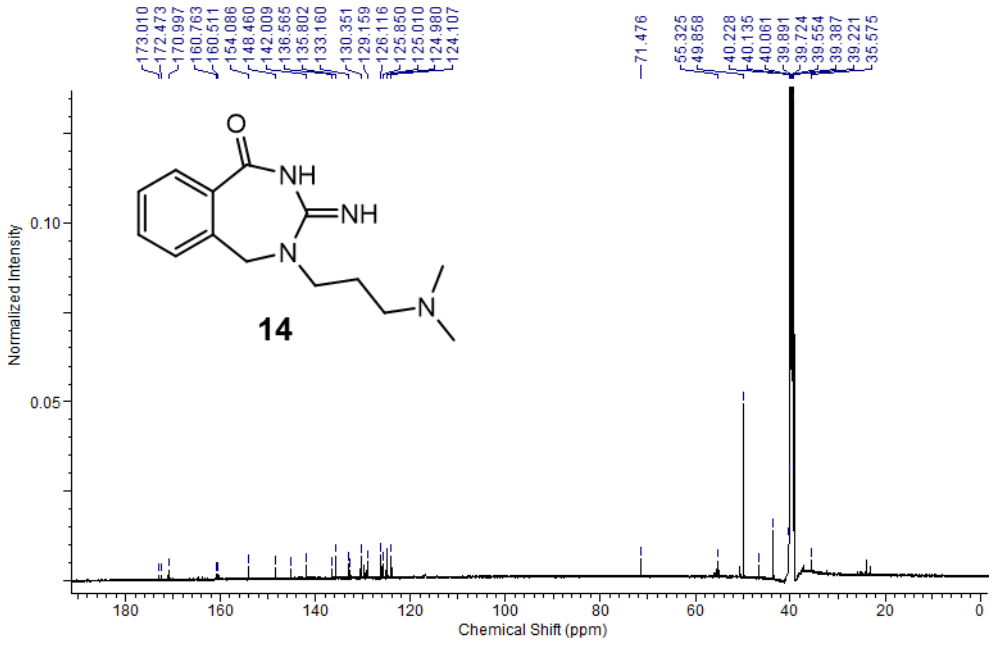

2.3 Dimethylquinazolinamine and spirocyclopropylquinazolinamines as new ligands targeting HCV IRES subdomain IIa

2.3.1 Synthesis of Dimethylquinazolinamine 15 and spirocyclopropylquinazolinamines 16 and 17 for targeting IRES subdomain IIa

The compound 4,4-dimethyl-3,4-dihydroquinazolin-2-amine **15** was envisioned to be synthesized with the commercially available 2-(2-aminopropan-2-yl)aniline in a one-pot double nucleophilic substitution to cyanogen bromide where the primary benzyl amine undergoes nucleophilic substitution to the bromine, then the aniline nuclephilically adds to the resulting imine carbon to form the intramolecular 6-memebered ring (**Scheme 2.3.1.1**).[41]

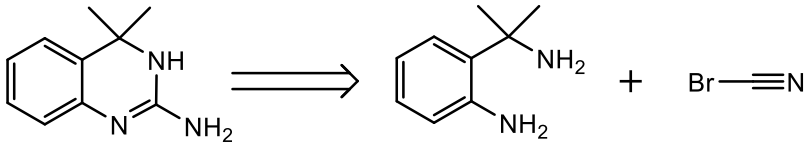

15

Scheme 2.3.1.1: Retrosynthetic analysis of dimethylquinazolinamine **15**.

The reaction proceeded readily when done is relatively dilute conditions, 0.05M, in Acetonitrile and cooled to 0°C to both decrease the chance of the multiple attacks of cyanogen bromide from two or more starting material molecule and then was allowed to warm to room temperature for intramolecular nucleophilic addition and closing of the 6-membered ring which would be the most favored in more dilute conditions (**Scheme 2.3.1.2**).

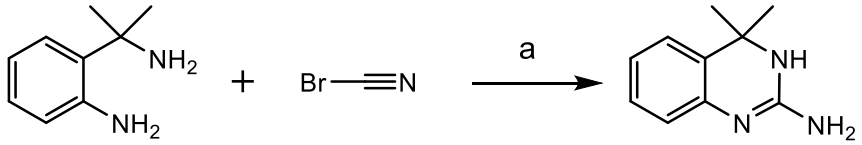

15

Scheme 2.3.1.2: Synthesis of dimethylquinazolinamine **15**.

Reagents and conditions: a) ACN, 0°C to R.T. over 4 hours, 97%.

Having this ring closing synthetic step work as well as it did for **15**, with a 97% yield, the spirocyclopropylquinazolinamines **16** and **17** were designed to be made in similar fashion. With the publication by P. Bertus and J. Szymoniak [37] allowing easier access to cyclopropyl compounds, specifically benzyl amines, if the ortho aniline could be established, as in compounds **27** and **28**, then the same cyanogen bromide ring closing reaction could be used to close the 6-memebered ring (**Scheme 2.3.1.3**).

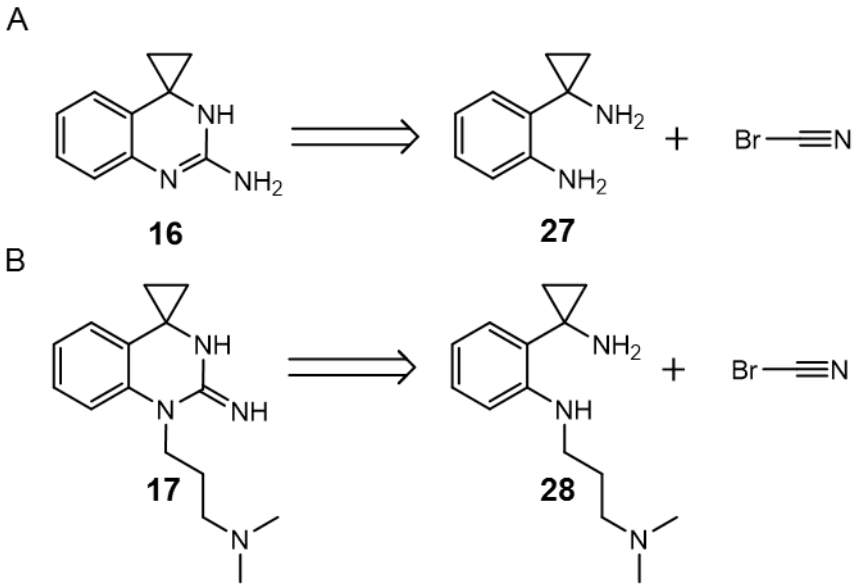

Scheme 2.3.1.3: The retrosynthetic analysis of spirocyclopropylquinazolinamines **16** and **17**. A) Retrosynthetic analysis of spirocyclopropylquinazolinamine **16** from **27**. B) Retrosynthetic analysis of spirocyclopropylquinazolinamine **17** from **28**.

The synthesis of the aminocyclopropylaniline **27** would be afforded from reduction of an ortho nitro group as in compound **29** which would be synthesized inspired by the publication by P. Bertus and J. Szymoniak [37] using a Szymoniak variation of the Kulinkovich reaction with commercially available 2-nitrobenzonitrile and ethyl magnesium bromide Grignard reagent (**Scheme 2.3.1.4**). The Grignard coordinates to Titanium(IV) Isopropoxide, this couples the nitrile and ethyl group together, and with the help of Lewis acid Boron trifluoride results in the cyclopropane group and connected benzyl primary amine.

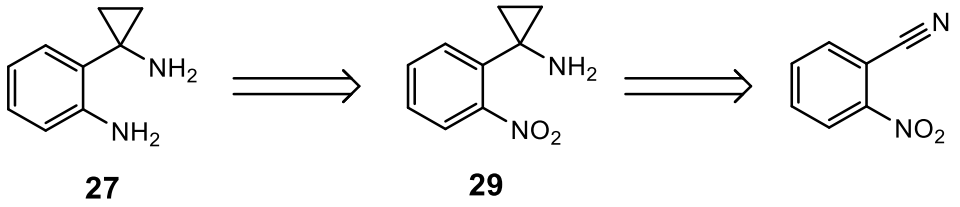

27 **29**

Scheme 2.3.1.4: Retrosynthetic analysis of aminocyclopropylaniline **27**.

Substituted aminocyclopropylaniline **28** could be synthesized using the same compound **29** by protection of the amine, reduction of the nitro group, nucleophilic substitution of commercially available 3-chloro-N,N-dimethylpropan-1-amine, and finally deprotection of the amine (**Scheme 2.3.1.5**).

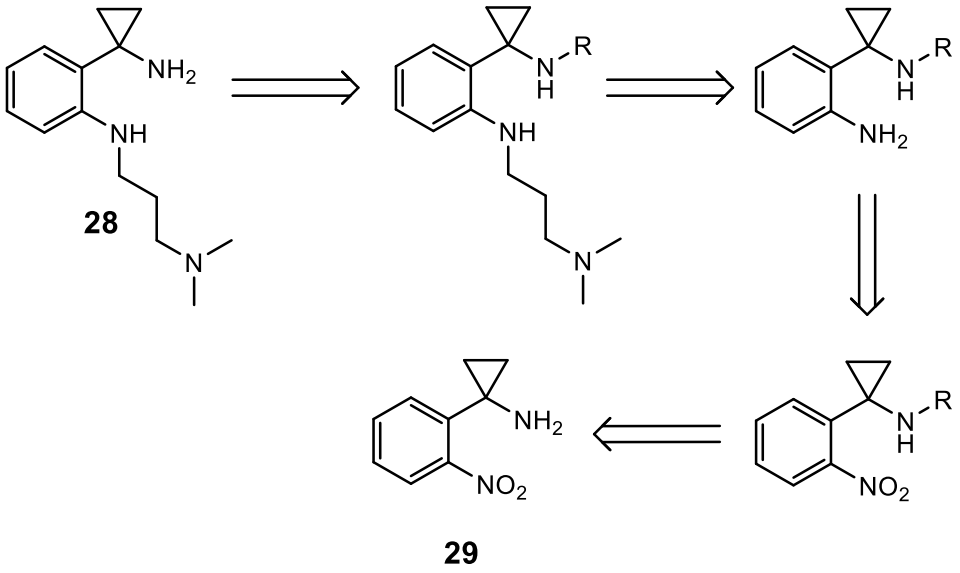

Scheme 2.3.1.5: Retrosynthetic analysis of substituted aminocyclopropylaniline **28** from **29**.

However, synthesis of 1-(2-nitrophenyl)cyclopropan-1-amine **29** did not yield the product as it is possible that the nitro group coordinates to the Titanium

metal, disrupting its ability to coordinate to the Grignard and/or starting material, and efforts to increase the amount of available Titanium catalyst to avoid this still did not result in the formation of product **29**. With the nitro group not tolerated in the reaction, the synthesis was altered to instead use the publication reaction product of 1-(2-bromophenyl)cyclopropan-1-amine **30** (**Scheme 2.3.1.6**).

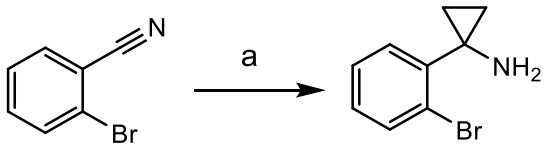

30

Scheme 2.3.1.6: Synthesis of 1-(2-bromophenyl)cyclopropan-1-amine **30**.

Reagents and conditions: Diethyl ether, Titanium (IV) Isopropoxide, -76°C, Ethyl Magnesium Bromide, warmed to R.T., Boron Trifluoride Etherate, HCl, NaOH, 90%.

The synthesis of 1-(2-bromophenyl)cyclopropan-1-amine **30** was afforded in good yield at 90% and the final products **16** and **17** were envisioned to be synthesized via nucleophilic aromatic substitution of 1-(2-bromophenyl)cyclopropan-1-amine **30** with commercially available amines ammonia and 3-(dimethylamino)-1-propylamine to aminocyclopropylanilines **27** and **28** respectively (**Scheme 2.3.1.7**).

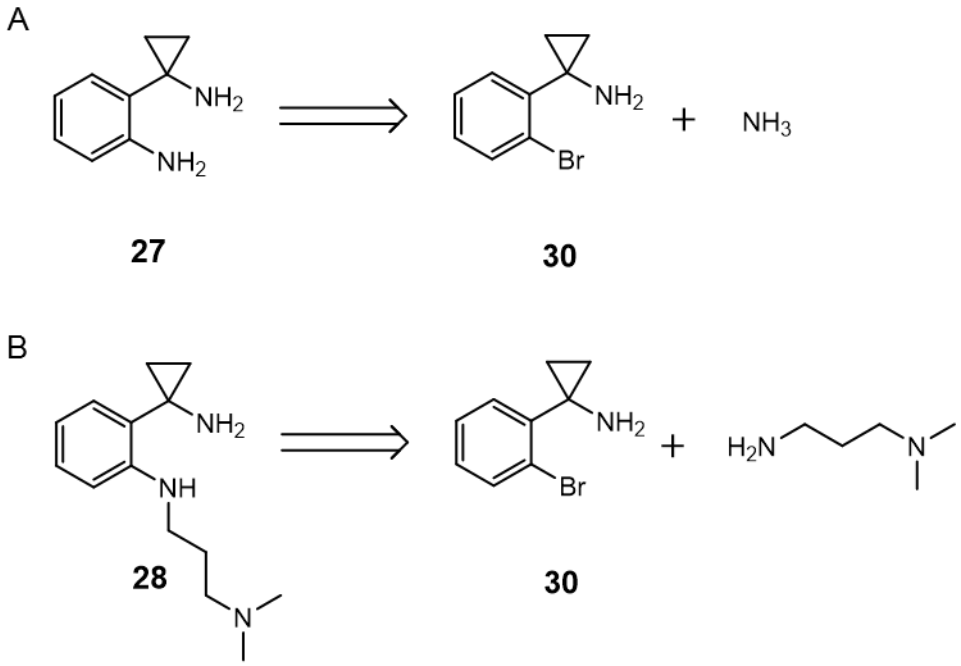

Scheme 2.3.1.7: The retrosynthetic analysis of aminocyclopropylanilines **27** and **28**. A) Retrosynthetic analysis of aminocyclopropylaniline **27** via nucleophilic aromatic substitution of **30** with ammonia. B) Retrosynthetic analysis of aminocyclopropylaniline **28** via nucleophilic aromatic substitution of **30** with 3-(dimethylamino)-1-propylamine.

From the aminocyclopropylanilines **27** and **28**, the final cyclization step would be done with cyanogen bromide in the same manner as the cyclization of dimethylquinazolinamine **15** (**Scheme 2.3.1.2**). Unfortunately, the nucleophilic substitutions were not successful, as side products and degradation occurred during the multiple attempts at the synthesis.

Typical nucleophilic substitution is done with withdrawing groups attached to the benzene ring in order to make the carbon more electrophilic and substitution to occur. The halide used can also make an impact in the substitution, as fluorines are better than bromines and iodines with its small

relative atomic size allowing the nucleophile better access to the benzene carbon. As the benzene ring of **30** did not have a withdrawing group other than the bromine itself it is understandable standard nucleophilic aromatic substitution conditions might not succeed. The fluorine derivative of **30**, 1-(2-fluorophenyl)cyclopropan-1-amine, was successfully synthesized using 2-fluorobenzonitrile in the exact same manner as **30** but the same nucleophilic aromatic substitution reactions attempted with **30** using 1-(2-fluorophenyl)cyclopropan-1-amine did not yield any product **27** or **28**. In an attempt to install a good withdrawing group to the ring, 2-bromo-5-nitrobenzonitrile was used in the cyclopropanation reaction, however the nitro group again did not allow the formation of the product.

Since nucleophilic aromatic substitution was unsuccessful, the substitution was envisioned to take place via a metal catalyzed cross coupling reaction. As the starting material had a free amine as well as the reaction with 3-(dimethylamino)-1-propylamine would create secondary amine as product, typical Buchwald-Hartwig cross coupling could create multiple side-products. A publication entitled: *“A facile and practical copper powder-catalyzed, organic solvent-and ligand-free Ullmann amination of aryl halides”* demonstrated the use of copper and copper oxide to cross couple amines to benzene rings with halides.[42] The advantages being the use of water and air as tolerable conditions in the reaction and more importantly secondary amines did not cross couple in the reaction. The resulting product **28** would not couple to another

starting material compound **30**. The reaction also had the best yields when done with a bromine halide. The reaction was tested and successful on a commercially available model compound 1-bromo-2-isopropylbenzene to yield N^1-(2-isopropylphenyl)-N^3,N^3-dimethylpropane-1,3-diamine in order to see if the amine 3-(dimethylamino)-1-propylamine would work in the cross coupling reaction (**Scheme 2.3.1.8**).

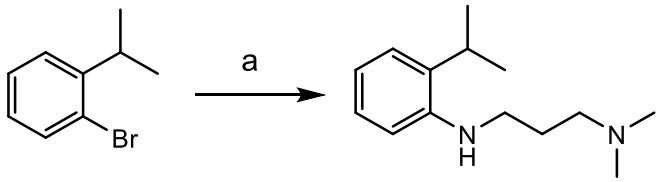

Scheme 2.3.1.8: The synthesis of N^1-(2-isopropylphenyl)-N^3,N^3-dimethylpropane-1,3-diamine from commercially available 1-bromo-2-isopropylbenzene.

Reagents and conditions: a) Cu_2O, ACN, 3-(dimethylamino)-1-propylamine, under argon, sealed tube, 100°C, 24 hours, 80%.

With confidence the 3-(dimethylamino)-1-propylamine would work in the cross coupling reaction, the two reactions using 1-(2-bromophenyl)cyclopropan-1-amine **30** and ammonia hydroxide and **30** with 3-(dimethylamino)-1-propylamine were attempted. As a small amount of product appeared in mass spec of the crude for the reaction of **30** with 3-(dimethylamino)-1-propylamine, the product was unable to be purified, as instead what was isolated was the substituted ethyl ketone 1-(2-((3-(dimethylamino)propyl)amino)phenyl)propan-1-one **31** (**Figure 2.3.1.1**).

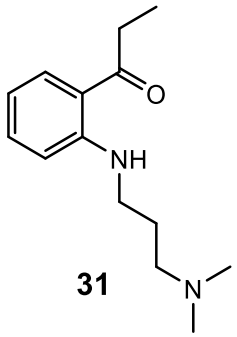

31

Figure 2.3.1.1: The structure of the unwanted side product **31** isolated based on NMR and mass spec from the cross coupling reaction of **30** with 3-(dimethylamino)-1-propylamine.

The addition of an ortho aniline group appeared to make the cyclopropyl group more unstable and sensitive to oxidation. Several attempts to synthesize the compound and isolate in a glove box with varying reaction durations and workup conditions never yielded clean product, and the addition of cyanogen bromide directly to the reaction mixture after 4 hours of cross coupling did not achieve the formation of **17**, instead only a small amount of unwanted side product seen by mass spec N-(3-(dimethylamino)propyl)-N-(2-propionylphenyl)cyanamide **32**, which is the result of the oxidized compound **31** undergoing nucleophilic substitution with cyanogen bromide (**Figure 2.3.1.2**).

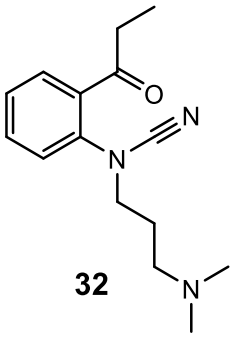

32

Figure 2.3.1.2: The structure of the unwanted side product **32** observed via mass spec as a result of oxidation then nucleophilic substitution with cyanogen bromide.

It was clear the aniline ortho to the cyclopropyl ring was unstable and the synthesis was redesigned to use cross coupling with commercially available cyanamide and **30** to form **33** which could be more stable but also undergo intramolecular nucleophilic addition to cyclize to the 6-membered ring product **16** under the reaction conditions (**Scheme 2.3.1.9**).

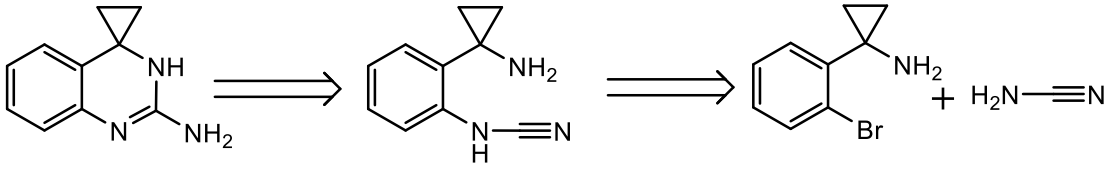

16 **33** **30**

Scheme 2.3.1.9: The retrosynthetic analysis of spirocyclopropylquinazolinamine **16**.

The synthesis of **16** was afforded via the same copper catalyzed coupling reaction conditions with 1-(2-bromophenyl)cyclopropan-1-amine **30** and cyanamide as the crude was analyzed via mass spectrometry and the product 3'H-spiro[cyclopropane-1,4'-quinazolin]-2'-amine **16** was found under hi-

resolution mass spec at a calculated $C_{10}H_{12}N_3$ $[M+H]^+$ = 174.1028 and found 174.1026 with a delta of 1.1 ppm. Purification using reverse-phase HPLC afforded a 20% yield of purified product as a yellow solid. The spirocyclopropylquinazolinamine was achieved when the two step, one pot reaction was attempted, as the ability to immediately form the 6-membered ring was important to avoid oxidation.

2.3.2 Testing of dimethylquinazolinamine 15 and spirocyclopropylquinazolinamines 16 and 17 as Ligands for Targeting HCV IRES subdomain IIa

The dimethylquinazolinamine **15** and spirocyclopropylquinazolinamine **16** were tested in the FRET assay which revealed good binding affinity of both compounds to the RNA target (**Table 2.3.2.1**).

Table 2.3.2.1: Ligand affinity of **15** and **16** measured by FRET assay. EC_{50} is the concentration required for a fifty percent reduction in the observed FRET signal.

Structure	FRET (EC_{50})
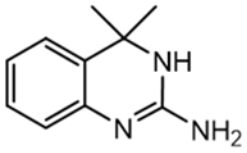 **15**	420 ± 60 µM
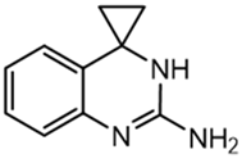 **16**	100 ± 30 µM

The fourfold better affinity of spirocyclopropylquinazolinamine **16** compared to dimethylquinazolinamine **15** suggests that the space filling effect of the substituent at the benzylic position plays an important role for ligand binding. The small change in space filling between the dimethyl and cyclopropyl groups resulted in a significant difference in binding affinity. It seems that the smaller cyclopropyl substituent provides a better fit for the ligand binding pocket than the slightly bulkier dimethyl group. Further design of compounds should focus on analogs carrying the cyclopropyl or a similarly sized sulfonyl group while the dimethyl group is likely too large for the binding pocket.

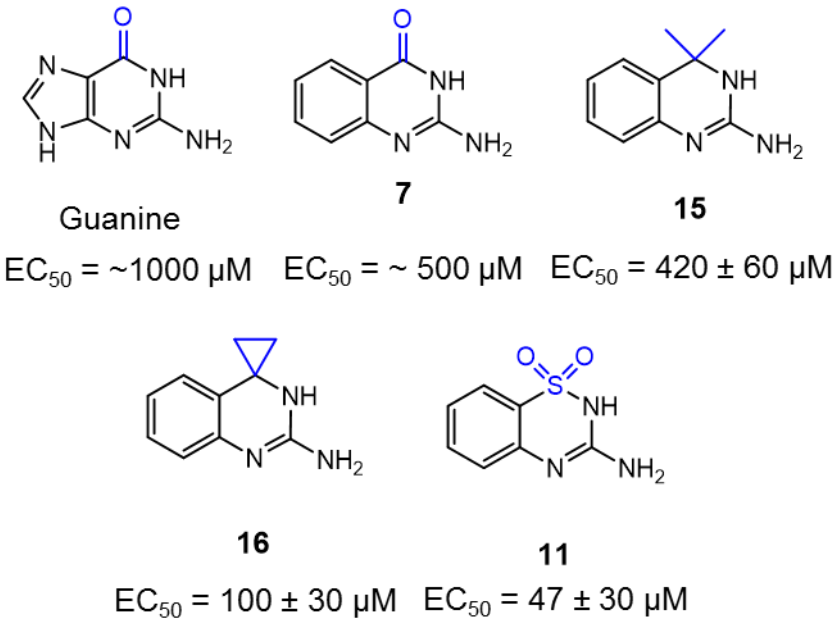

Figure 2.3.2.1: The overview of Guanine, its derivatives, and their respective FRET data.

To summarize the implications of these findings (**Figure 2.3.2.1**), replacing the quinazolinone **7** carbonyl group with a dimethyl group, as in **15**, an increase in FRET is observed. However, when replaced with the cyclopropyl group as in **16**, we see nearly a fivefold increase in binding affinity. Replacing the carbonyl with the sulfonyl as with the benzothiadiazine **11**, we see a tenfold increase in binding affinity but only a twofold increase compared to the spirocyclopropylquinazolinamine **16**. The change in planarity appears more important to binding to the subdomain IIa than the polarity or hydrogen bonding ability of the sulfonyl oxygens. Clearly, the size of the nonplanar substituent (dimethyl vs. cyclopropyl) was shown to be significant. Also, the polarity and ability to hydrogen bond the sulfonyl group does make a positive impact in

binding, as a twofold increase in binding is seen when comparing the spirocyclopropylquinazolinamine **16** to the benzothiadiazine **11**. it is best to have a space filling group similar to the size of the cyclopropyl or sulfonyl but also have polar groups like oxygen attached. Derivatives of the spirocyclopropylquinazolinamines and the benzothiadiazines may be promising future synthesis targets to further increase potency of ligands binding to the HCV subdomain IIa that could be used in combination therapy or eventually as a singular cure to all genotypes of HCV.

2.3.3 Materials and Methods

4,4-dimethyl-3,4-dihydroquinazolin-2-amine (15)

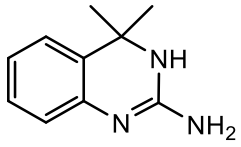

15

Figure 2.3.3.1: 4,4-dimethyl-3,4-dihydroquinazolin-2-amine (**15**).

A solution of 2-(2-Amino-2-propyl) aniline (1.13 mmol, 0.169 g) in 20 mL of acetonitrile was purged with argon gas, magnetically stirred, and cooled to 0°C via an ice bath, where a premade solution of Cyanogen Bromide in acetonitrile (25.77 mmol, 2.730 g, in 10 mL of acetonitrile, giving 2.58 M concentration) was added (1.24 mmol, 0.484 mL) dropwise. This was allowed to warm to room temperature overnight via ambient atmospheric temperature and monitored via thin layer chromatography. The solvent was removed *in vacuo* giving a yellow oil. This was purified using reverse-phase HPLC at a gradient of 0.2%-25% acetonitrile in water to give **15** as a yellow oil in a purified yield of 97%.[41]

15: ^{1}H NMR (500 MHz, DMSO-d_6) δ 10.617 (br s, 1H, NH), 8.616 (br s, 1H, NH), 7.375 (d, 1H, J = 8.0 Hz), 7.278 (t, 1H, J = 7.5 Hz), 7.135 (t, 1H, J = 8.5 Hz), 7.011 (d, 1H, J = 8 Hz), 1.533 (s, 6H); ^{13}C NMR (500 MHz, DMSO-d_6) δ 151.203,

131.753, 128.892, 127.412, 124.995, 124.965, 115.860, 53.881, 30.830; HRMS mass calculated $C_{10}H_{14}N_3$ $[M+H]^+$ = 176.1182 , found 176.1183; Delta 0.6 ppm.

1-(2-bromophenyl)cyclopropan-1-amine (30)

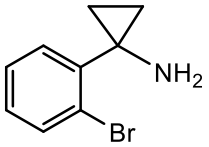

30

Figure 2.3.3.2: 1-(2-bromophenyl)cyclopropan-1-amine (**30**).

2-bromo-benzonitrile (1.00 mmol, 0.182 g) was dissolved in 50mL of diethyl ether under argon and Titanium (IV) Isopropoxide (1.10 mmol, 0.330 mL) was added at room temperature and stirred via magnetic stirring. The mixture was cooled to -76°C. Ethyl magnesium bromide, where a 3 M Ethyl Magnesium Bromide solution in diethyl ether (2.20 mmol, 0.730 mL) was added dropwise. This was allowed to stir for 40 minutes, where it was removed from the dry ice/acetone bath and allowed to come to room temperature. Boron Triflouride Etherate (2.00 mmol, 0.250 mL) was added and the solution became dark brown. This was allowed to stir for 1 hour. 3 mL of 1N HCl (aq) was added and allowed to stir for another 20 minutes. 10 mL of 10% NaOH (aq) was added and blue precipitate forms. The organic layer was extracted, dried over $MgSO_4$, and the solvent was removed *in vacuo* to give a light yellow crude oil. Flash

Chromatography using silica gel (1:1 hexanes/ethyl acetate) afforded **30** as a yellow oil at 90% yield.[37]

30: ^{1}H NMR (500 MHz, $CDCl_3$) δ 7.555 (dd, 1H, J = 8.0 Hz, J' = 1 Hz), 7.363 (dd, 1H, J = 7.5 Hz, J' = 2 Hz), 7.243 (dt, 1H, J = 7.0 Hz, J' = 1 Hz), 7.096 (dt, 1H, J = 7.5 Hz, J' = 2 Hz), 2.334 (br s, 2H, NH_2), 1.093 (dd, 1H, J = 6.8 Hz, J' = 4.5 Hz), 0.916 (dd, 1H, J = 6.8 Hz, J' = 4.5 Hz); ^{13}C NMR (500 MHz, $CDCl_3$) δ 144.443, 133.002, 130.097, 128.350, 127.410, 125.311, 38.667, 15.331; HRMS mass calculated $C_9H_{11}BrN$ $[M+H]^+$ = 212.0069, found 212.0069; Delta 0.0 ppm.

3'H-spiro[cyclopropane-1,4'-quinazolin]-2'-amine (16)

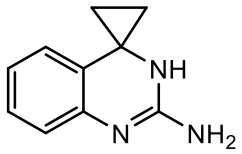

16

Figure 2.3.3.3: 3'H-spiro[cyclopropane-1,4'-quinazolin]-2'-amine (**16**).

1-(2-bromophenyl)cyclopropan-1-amine (1.04 mmol, 0.220 g) in 1 mL of acetonitrile was transferred into a 10 mL sealed tube, where cat. Cu_2O (15% by mol%, 0.156 mmol, 0.0224 g) was added, cyanamide (2.08 mmol, 0.088 g), and flushed with argon gas under magnetic stirring. This mixture was heated to 100°C in and oil bath for 18 hours where it was cooled to room temp and filtered. The solvent was removed *in vacuo* and resulted in a yellow oil. This was purified

using reverse-phase HPLC at a gradient of 0.2%-60% acetonitrile in water to give **16** as a yellow solid in a purified yield of 20%.[42]

16: ^{1}H NMR (500 MHz, CD_3CN) δ 10.153 (br s, 1H, NH), 8.166 (d, 1H, J = 8.0 Hz) 7.917 (t, 1H, J = 8.0 Hz), 7.629 (d, 1H, J = 8.0 Hz), 7.521 (t, 1H, J = 7.5 Hz), 7.130 (br s, 1H, NH), 6.552 (br s, 1H, NH), 1.862 (s, 2H), 0.880 (s, 2H); ^{13}C NMR (500 MHz, CD_3CN) δ 175.858, 161.072, 152.818, 134.883, 126.529, 126.429, 123.68, 61.282, 28.264; HRMS mass calculated $C_{10}H_{12}N_3$ $[M+H]^+$ = 174.1027, found 174.1026; Delta 0.6 ppm.

2.3.4 Spectral Data

Nuclear Magnetic Resonance

Spectrum 2.3.4.1: 4,4-dimethyl-3,4-dihydroquinazolin-2-amine (**15**) ^{1}H NMR (500MHz, DMSO-d_6).

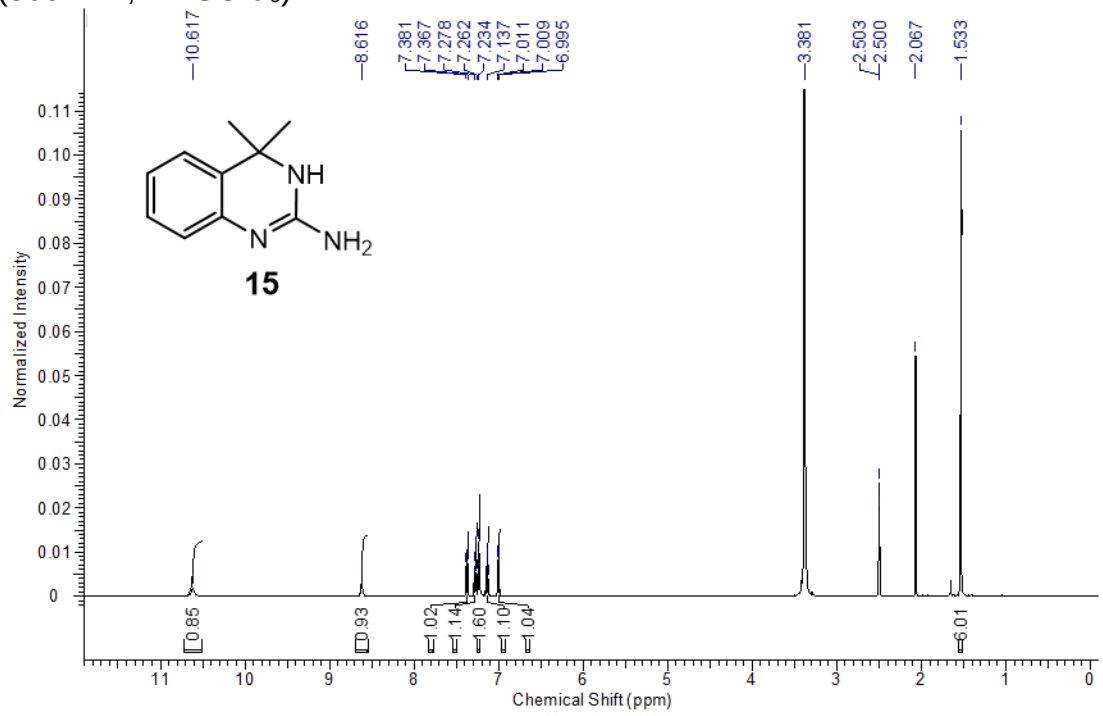

Spectrum 2.3.4.2: 4,4-dimethyl-3,4-dihydroquinazolin-2-amine (**15**) ^{13}C NMR (500MHz, DMSO-d_6).

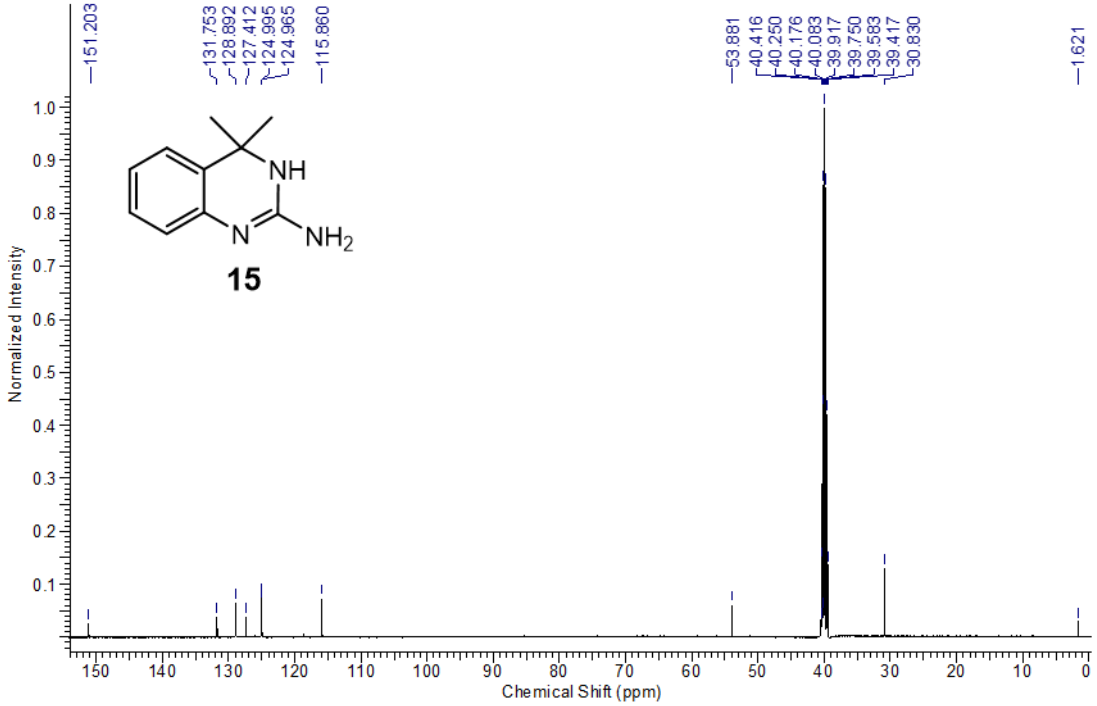

Spectrum 2.3.4.3: 1-(2-bromophenyl)cyclopropan-1-amine (**30**) ^{1}H NMR (500MHz, $CDCl_3$).

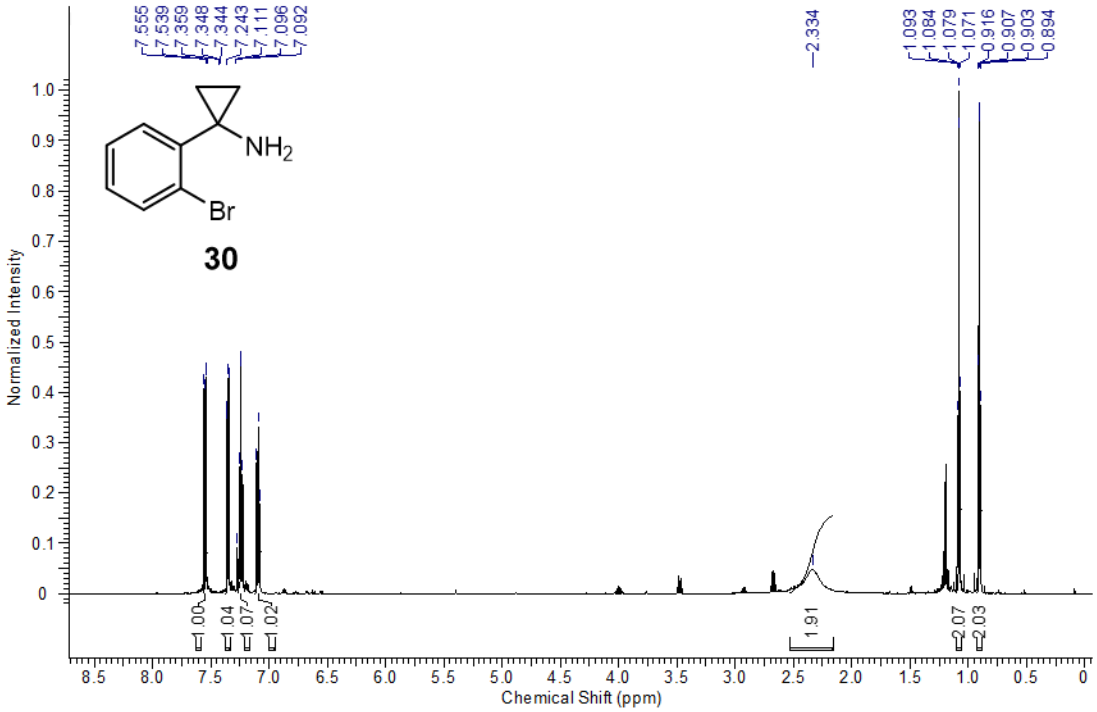

Spectrum 2.3.4.4: 1-(2-bromophenyl)cyclopropan-1-amine (**30**) ^{13}C NMR (500MHz, $CDCl_3$).

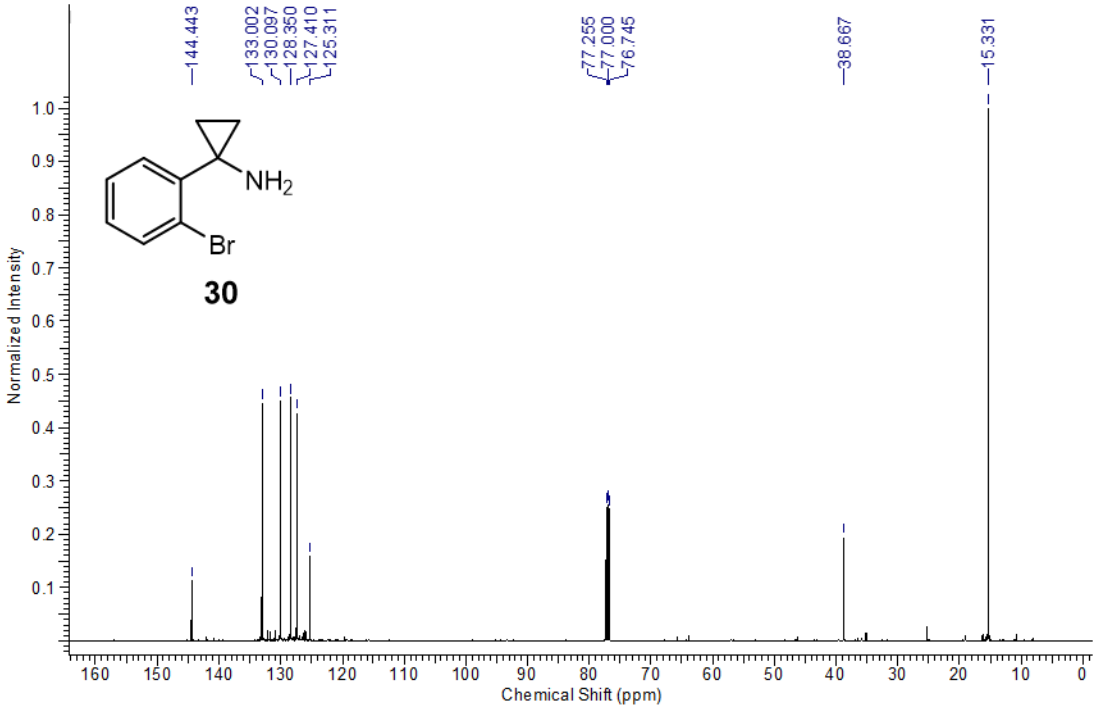

Spectrum 2.3.4.5: 3'H-spiro[cyclopropane-1,4'-quinazolin]-2'-amine (**16**) ^{1}H NMR (500MHz, CD_3CN).

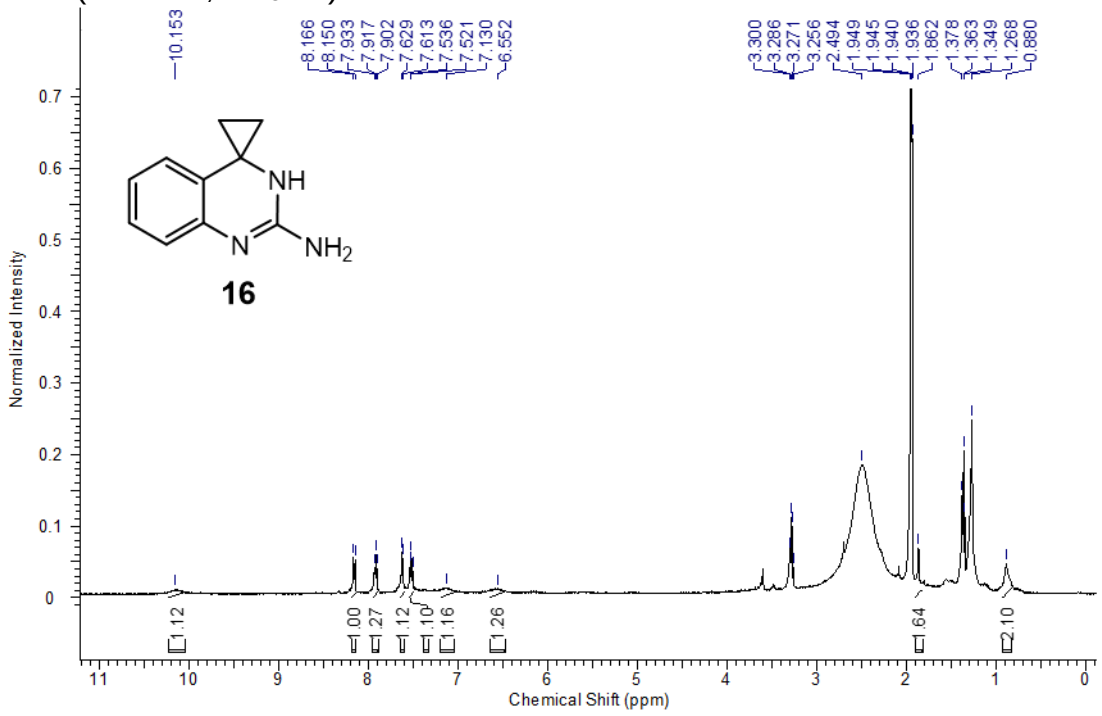

Spectrum 2.3.4.6: 3'H-spiro[cyclopropane-1,4'-quinazolin]-2'-amine (**16**) ^{13}C NMR (500MHz, CD_3CN).

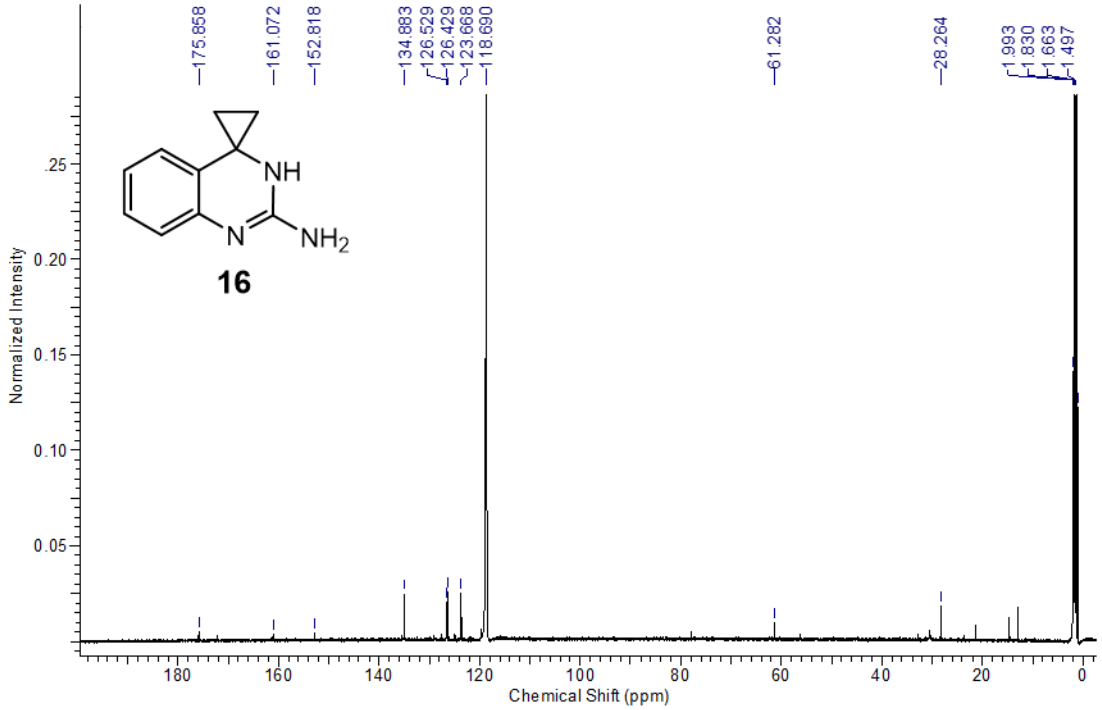

References

[1] T. R. Cech and J. A. Steitz, “The Noncoding RNA Revolution— Trashing Old Rules to Forge New Ones,” *Cell*, vol. 157, pp. 77–94, 2014.

[2] L. S. McCoy, Y. Xie, and Y. Tor, “Antibiotics that target protein synthesis.,” *Wiley Interdiscip. Rev. RNA*, vol. 2, no. 2, pp. 209–32.

[3] S. F. J. Le Grice, “Targeting the HIV RNA Genome: High-Hanging Fruit Only Needs a Longer Ladder,” Springer International Publishing, 2015, pp. 147–169.

[4] S. M. Dibrov, J. Parsons, M. Carnevali, S. Zhou, K. D. Rynearson, K. Ding, E. G. Sega, N. D. Brunn, M. A. Boerneke, M. P. Castaldi ||, and T. Hermann, “Hepatitis C Virus Translation Inhibitors Targeting the Internal Ribosomal Entry Site,” *J. Med. Chem.*, vol. 57, no. 5, pp. 1694–1707, 2014.

[5] D. Matzner and G. Mayer, “(Dis)similar Analogues of Riboswitch Metabolites as Antibacterial Lead Compounds,” *J. Med. Chem.*, vol. 58, no. 8, pp. 3275–3286, Apr. 2015.

[6] M. J. Alter, D. Kruszon-Moran, O. V. Nainan, G. M. McQuillan, F. Gao, L. A. Moyer, R. A. Kaslow, and H. S. Margolis, “The Prevalence of Hepatitis C Virus Infection in the United States, 1988 through 1994,” *N. Engl. J. Med.*, vol. 341, no. 8, pp. 556–562, Aug. 1999.

[7] S. M. Dibrov, K. Ding, N. D. Brunn, M. a. Parker, B. M. Bergdahl, D. L. Wyles, and T. Hermann, “Structure of a hepatitis C virus RNA domain in complex with a translation inhibitor reveals a binding mode reminiscent of riboswitches,” *Proc. Natl. Acad. Sci.*, vol. 109, no. 14, pp. 5223–5228, 2012.

[8] H. R. Rosen, “Chronic Hepatitis C Infection,” *N. Engl. J. Med.*, vol. 364, no. 25, pp. 2429–2438, Jun. 2011.

[9] B. R. Edlin, B. J. Eckhardt, M. A. Shu, S. D. Holmberg, and T. Swan, “Toward a more accurate estimate of the prevalence of hepatitis C in the United States.,” *Hepatology*, vol. 62, no. 5, pp. 1353–63, Nov. 2015.

[10] M. M. Denniston, R. B. Jiles, J. Drobeniuc, R. M. Klevens, J. W. Ward, G. M. Mcquillan, and S. D. Holmberg, “Chronic Hepatitis C Virus Infection in the United States, National Health and Nutrition Examination Survey 2003 to 2010.”

[11] K. N. Ly, J. Xing, R. M. Klevens, R. B. Jiles, J. W. Ward, and S. D.

Holmberg, “The increasing burden of mortality from viral hepatitis in the United States between 1999 and 2007.,” *Ann. Intern. Med.*, vol. 156, no. 4, pp. 271–8, Feb. 2012.

[12] American Association For The Study Of Liver Diseases, “Recommendations for Testing, Managing, and Treating Hepatitis C,” 2016.

[13] A. F. Luetkemeyer and D. L. Wyles, “CROI 2015: Highlights of Viral Hepatitis Therapy.,” *Top. Antivir. Med.*, vol. 23, no. 1, pp. 66–76.

[14] R. T. Chung, G. L. Davis, D. M. Jensen, H. Masur, M. S. Saag, D. L. Thomas, A. I. Aronsohn, M. R. Charlton, J. J. Feld, R. J. Fontana, M. G. Ghany, E. W. Godofsky, C. S. Graham, A. Y. Kim, J. J. Kiser, S. Kottilil, K. M. Marks, P. Martin, K. Mitruka, T. R. Morgan, S. Naggie, D. Raymond, N. S. Reau, R. T. Schooley, K. E. Sherman, M. S. Sulkowski, H. E. Vargas, J. W. Ward, and D. L. Wyles, “Hepatitis C Guidance: AASLD-IDSA Recommendations for Testing, Managing, and Treating Adults Infected with Hepatitis C Virus.,” *Hepatology*, vol. 62, no. 3, pp. 932–54, Jun. 2015.

[15] J. J. Feld and J. H. Hoofnagle, “Mechanism of action of interferon and ribavirin in treatment of hepatitis C.,” *Nature*, vol. 436, no. 7053, pp. 967–72, Aug. 2005.

[16] M. G. Ghany, D. R. Nelson, D. B. Strader, D. L. Thomas, L. B. Seeff, and American Association for Study of Liver Diseases, “An update on treatment of genotype 1 chronic hepatitis C virus infection: 2011 practice guideline by the American Association for the Study of Liver Diseases.,” *Hepatology*, vol. 54, no. 4, pp. 1433–44, Oct. 2011.

[17] M. Robinson, Y. Tian, W. E. Delaney, and A. E. Greenstein, “Preexisting drug-resistance mutations reveal unique barriers to resistance for distinct antivirals,” *Proc. Natl. Acad. Sci.*, vol. 108, no. 25, pp. 10290–10295, Jun. 2011.

[18] O. Vidalin, M. E. Major, B. Rayner, J. L. Imbach, C. Trépo, and G. Inchauspé, “In vitro inhibition of hepatitis C virus gene expression by chemically modified antisense oligodeoxynucleotides.,” *Antimicrob. Agents Chemother.*, vol. 40, no. 10, pp. 2337–44, Oct. 1996.

[19] Q. L. Choo, K. H. Richman, J. H. Han, K. Berger, C. Lee, C. Dong, C. Gallegos, D. Coit, R. Medina-Selby, and P. J. Barr, “Genetic organization and diversity of the hepatitis C virus.,” *Proc. Natl. Acad. Sci. U. S. A.*, vol.

88, no. 6, pp. 2451–5, Mar. 1991.

[20] C. S. Fraser and J. a Doudna, “Structural and mechanistic insights into hepatitis C viral translation initiation.,” *Nat. Rev. Microbiol.*, vol. 5, no. 1, pp. 29–38, 2007.

[21] N. Quade, D. Boehringer, M. Leibundgut, J. Van Den Heuvel, and N. Ban, “Cryo-EM structure of Hepatitis C virus IRES bound to the human ribosome at 3.9-Å resolution,” *Nat. Commun.*, vol. 6, 2015.

[22] G. A. Otto and J. D. Puglisi, “The Pathway of HCV IRES-Mediated Translation Initiation,” *Cell*, vol. 119, no. 3, pp. 369–380, 2004.

[23] H. Ji, C. S. Fraser, Y. Yu, J. Leary, and J. A. Doudna, “Coordinated assembly of human translation initiation complexes by the hepatitis C virus internal ribosome entry site RNA.,” *Proc. Natl. Acad. Sci. U. S. A.*, vol. 101, no. 49, pp. 16990–5, Dec. 2004.

[24] J. S. Kieft, A. Grech, P. Adams, and J. A. Doudna, “Mechanisms of internal ribosome entry in translation initiation.,” *Cold Spring Harb. Symp. Quant. Biol.*, vol. 66, pp. 277–83, 2001.

[25] C. U. Hellen and T. V Pestova, “Translation of hepatitis C virus RNA.,” *J. Viral Hepat.*, vol. 6, no. 2, pp. 79–87, Mar. 1999.

[26] M. A. Boerneke, S. M. Dibrov, J. Gu, D. L. Wyles, and T. Hermann, “Functional conservation despite structural divergence in ligand-responsive RNA switches.,” *Proc. Natl. Acad. Sci. U. S. A.*, vol. 111, no. 45, pp. 15952–7, 2014.

[27] P. J. Lukavsky, “Structure and function of HCV IRES domains,” *Virus Res.*, vol. 139, no. 2, pp. 166–171, 2009.

[28] P. P. Seth, A. Miyaji, E. A. Jefferson, K. A. Sannes-lowery, S. A. Osgood, S. S. Propp, R. Ranken, C. Massire, R. Sampath, D. J. Ecker, E. E. Swayze, and R. H. Griffey, “SAR by MS : Discovery of a New Class of RNA-Binding Small Molecules for the Hepatitis C Virus : Internal Ribosome Entry Site IIA Subdomain RNA-Binding Small Molecules for the Hepatitis C Virus : Internal Ribosome Entry Site IIA Subdomain,” *J. Med. Chem.*, pp. 7099–7102, 2005.

[29] J. Parsons, M. P. Castaldi, S. Dutta, S. M. Dibrov, D. L. Wyles, and T. Hermann, “Conformational inhibition of the HCV IRES RNA,” *Nat Chem Biol.*, vol. 5, no. 11, pp. 823–825, 2009.

[30] S. Zhou, K. D. Rynearson, K. Ding, N. D. Brunn, and T. Hermann, “Screening for inhibitors of the hepatitis C virus internal ribosome entry site RNA.”

[31] M. A. Boerneke and T. Hermann, “Conformational flexibility of viral RNA switches studied by FRET,” 2015.

[32] M. A. Parker, E. Satkiewicz, T. Hermann, and B. M. Bergdahl, “An efficient new route to dihydropyranobenzimidazole inhibitors of HCV replication,” *Molecules*, vol. 16, no. 1, pp. 281–290, 2011.

[33] Adrien Albert, R. Goldacre, and J. Phillips, “The Strength of Heterocyclic Bases,” *J. Chem. Soc.*, pp. 2240–2249, 1948.

[34] K. D. Rynearson, B. Charrette, C. Gabriel, J. Moreno, M. A. Boerneke, S. M. Dibrov, and T. Hermann, “2-Aminobenzoxazole ligands of the hepatitis C virus internal ribosome entry site,” *Bioorg. Med. Chem. Lett.*, vol. 24, pp. 3521–3525, 2014.

[35] T. Janas, J. J. Widmann, R. Knight, and M. Yarus, “Simple, recurring RNA binding sites for L-arginine.”

[36] H. Sajiki, T. Ikawa, and K. Hirota, “Reductive and Catalytic Monoalkylation of Primary Amines Using Nitriles as an Alkylating Reagent.”

[37] P. Bertus and J. Szymoniak, “A direct synthesis of 1-aryl- and 1-alkenylcyclopropylamines from aryl and alkenyl nitriles,” *J. Org. Chem.*, vol. 68, no. 18, pp. 7133–7136, 2003.

[38] M. Tandon, Y. Liu, N. Namdev, M. A. Ashwell, and P. Rocio, “Substituted dipyrido-pyrimido-diazepine and benzo-pyrido-pyrimido compounds,” US 2010/0249108 A1, 2010.

[39] C. K. Lee, J. S. Yu, and Y. R. Ji, “Determination of Aromaticity Indices of Thiophene and Furan by Nuclear Magnetic Resonance Spectroscopic Analysis of Their Anilides,” *J. Heterocycl. Chem.*, vol. 39, pp. 1219–1227, 2002.

[40] M. Ikejiri, K. Matsumoto, H. Hasegawa, D. Yamaguchi, M. Tsuchino, Y. Chihara, T. Yamaguchi, K. Mori, T. Imanishi, S. Obika, and K. Miyashita, “Synthesis and fluorescence properties of 4-diarylmethylene analogues of the green fluorescent protein chromophore,” *Tetrahedron*, vol. 71, no. 30, pp. 4987–4998, 2015.

[41] F. Ishikawa, Y. Watanabe, and J. Saugusa, “Cyclic Guanidines. IX. Synthesis of 2-Amino-3,4-dihydroquinazolines as Blood Platelet Aggregation Inhibitors,” *Chem Pharm Bull*, vol. 28, no. 1980, pp. 1357–1364, 1979.

[42] J. Jiao, X. R. Zhang, N. H. Chang, J. Wang, J. F. Wei, X. Y. Shi, and Z. G. Chen, “A facile and practical copper powder-catalyzed, organic solvent-and ligand-free Ullmann amination of aryl halides,” *J. Org. Chem.*, vol. 76, no. 4, pp. 1180–1183, 2011.